IDENTIFYING TARGETS AND FUNCTION OF THE UBIQUITIN RELATED MODIFIER URM1 IN *SACCHAROMYCES CEREVISIAE*

by

CHARLES E. KUBICEK

A DISSERTATION

Presented to the Department of Biology
and the Graduate School of the University of Oregon
in partial fulfillment of the requirements
for the degree of
Doctor of Philosophy

September 2009

University of Oregon Graduate School

Confirmation of Approval and Acceptance of Dissertation prepared by:

Charles Kubicek

Title:

"Identifying targets and function of the Ubiquitin Related Modifier Urm1 in Saccharomyces cerevisiae"

This dissertation has been accepted and approved in partial fulfillment of the requirements for the Doctor of Philosophy degree in the Department of Biology by:

Karen Guillemin, Chairperson, Biology
George Sprague, Advisor, Biology
Alice Barkan, Member, Biology
Kenneth Prehoda, Member, Chemistry
Tom Stevens, Outside Member, Chemistry

and Richard Linton, Vice President for Research and Graduate Studies/Dean of the Graduate School for the University of Oregon.

September 5, 2009

Original approval signatures are on file with the Graduate School and the University of Oregon Libraries.

An Abstract of the Dissertation of

Charles E. Kubicek for the degree of Doctor of Philosophy

in the Department of Biology to be taken September 2009

Title: IDENTIFYING TARGETS AND FUNCTION OF THE UBIQUITIN RELATED MODIFIER URM1 IN *SACCHAROMYCES CEREVISIAE*

Approved: _____
Dr. George Sprague

Post-translational modification of proteins is an important cellular method of controlling various aspects of protein activity, including protein-protein interactions, half-life, and transport. An important class of post-translational modifications involves the ubiquitin family of proteins. In these modifications, a small protein, such as ubiquitin, is conjugated to a target protein through an isopeptide bond. Conjugation by a ubiquitin family member acts as a signal to regulate the activity, function, or stability of the target protein. Urm1, a ubiquitin-like protein conserved throughout all eukaryotes, was initially identified in *S. cerevisiae*. Loss of Urm1 leads to the disruption of a variety of cellular processes, including oxidative stress response, filamentous growth, and temperature sensitivity. This body of work comprises efforts to identify novel targets of Urm1, the mechanism by which Urm1 is attached to target proteins, and the physiological consequences of such conjugation.

To gain understanding of the function and mechanism of Urm1 conjugation, the only known conjugate of Urm1, the peroxiredoxin reductase Ahp1, was examined in an effort to identify the site of modification on Ahp1 and to evaluate the physiological consequences of urmylation of Ahp1. I then completed a series of screens - a synthetic lethal screen, a two-hybrid screen, and a protein over-expression screen - to identify

novel Urm1 conjugates and cellular functions dependent on Urm1. Of particular interest were genes identified in the synthetic lethal screen, namely *PTC1*, which encodes a protein phosphatase, and a set of genes encoding the Elongator complex, which functions in transcriptional elongation and tRNA modification.

During this time period, other groups showed that thiolation of tRNAs depends on Urm1. Thus, Urm1 does not function only in protein conjugation, but also as a sulfur carrier in the thiolation of tRNA. Interestingly, I identified Elp2, a component of the Elongator complex, as a new Urm1-conjugate. Because Elp2 is also required for tRNA modification, perhaps Urm1 plays more than one role in tRNA modification. Loss of tRNA modification may disrupt many cellular functions and could explain the variety of *urm1* mutant phenotypes. I have determined that all known Urm1 dependent processes are also associated with tRNA modification.

CURRICULUM VITAE

NAME OF AUTHOR: Charles E. Kubicek

PLACE OF BIRTH: Corpus Christi, Texas

DATE OF BIRTH: March 5, 1981

GRADUATE AND UNDERGRADUATE SCHOOLS ATTENDED:

University of Oregon, Eugene
Georgia Institute of Technology, Atlanta

DEGREES AWARDED:

Doctor of Philosophy, Biology, 2009, University of Oregon
Bachelor of Science in Biology, 2003, Georgia Institute of Technology

AREAS OF SPECIAL INTEREST:

Genetics
Molecular Biology

PROFESSIONAL EXPERIENCE:

Graduate Research Assistant, Institute of Molecular Biology
University of Oregon, 2003-2009

Graduate Teaching Assistant, Department of Biology
University of Oregon, 2003-2004

Undergraduate Research Assistant, Department of Biology
Georgia Institute of Technology, 2000-2003

GRANTS, AWARDS AND HONORS:

National Institute of Health Molecular Biology Pre-doctoral training grant
University of Oregon, 2005-2006

Howard Hughes Fellowship
Georgia Institute of Technology, 2001

TABLE OF CONTENTS

Chapter Page

LIST OF FIGURES

Figure Page

Figure Page

LIST OF TABLES

Table Page

CHAPTER I

AN INTRODUCTION TO THE UBIQUITIN-LIKE SYSTEM, URMYLATION

The function of proteins is often regulated by post-translational modification. In many cases the modification is a small moiety such as a phosphate group but in some cases the modification is a peptide. The archetypical example of this latter type is ubiquitin, a 98 amino acid peptide conserved throughout the eukaryotic world. Ubiquitination of proteins was first shown to regulate their stability, but more recent work has shown that ubiquitination can regulate other aspects of protein function. In recent years several other ubiquitin-like peptide modifiers have been identified. The members of this so-called ubiquitin-family, though only moderately similar in sequence, share a similar size and a C-terminal glycine-glycine motif that serves as the point of covalent attachment to lysine residues in the target protein. In this chapter I will first summarize the enzymatic steps involved in activating and attaching ubiquitin and the members of the family, ubiquitin-like proteins (Ubl), to target proteins, then discuss the different Ubls and what is known about their functions, and finally focus on Urm1, the newest Ubl and the subject of this study.

The Ubiquitin Family of Proteins

In the ubiquitin system, ubiquitin is conjugated to the target protein in three enzymatic steps. First, ubiquitin forms a thioester bond to the E1 activating enzyme. Ubiquitin is then transferred to the E2 conjugating enzyme through another thioester bond. Finally, the E2 conjugating and E3 ligase enzymes attach ubiquitin via its C-terminal glycine to the lysine of the target protein (Kerscher *et al.*, 2006). A target protein may be mono-ubiquitinated or poly-ubiquitinated (ubiquitin can conjugate to other ubiquitin moieties to form a chain off the target protein) (Kerscher *et al.*, 2006)

Poly-ubiquitination of a target was initially identified as a signal for degradation via the proteasome, however other forms of ubiquitin chains can trigger other outcomes such as promoting interaction with signal transduction pathways, DNA repair, or endocytosis (Ciechanover *et al.*, 1994; Di Fiore *et al.*, 2003; Matunis *et al.*, 2002). Mono-ubiquitination also plays a role in other processes such as transport through the multivesicular body and histone modification (Haglund *et al.*, 2003; Bach *et al.*, 2003).

What is the consequence of attaching ubiquitin to a protein? Ubiquitin can provide a new surface for protein-protein interactions; proteins that recognize the conjugated ubiquitin will often have a consensus ubiquitin-binding domain (UBD) (Hicke *et al.*, 2005). These new protein interactions can then change the activity or localization of the conjugated protein (Hicke *et al.*, 2005). Ultimately the ubiquitin signal controls a large variety of cellular process from cell cycle control, general degradation events, DNA repair, vesicle trafficking, endocytosis and viral budding (Di Fiore *et al.*, 2003).

Several other ubiquitin like proteins, Ubls, have been identified and characterized in yeast and other organisms: Sumo, Nedd8, and Apg12. Like ubiquitin, Ubls are small proteins and share a general domain structure, most notably the C-terminal glycine-glycine motif required for conjugation to the target. The conjugation of these Ubls follows the same mechanism as for ubiquitin, each with their own E1-E3 enzymes, that attach the Ubls to lysines on the target (Hochstrasser *et al.*, 2000). While the mechanism of attachment and structure of each of the Ubls is similar to ubiquitin, the resulting consequence of conjugation is varied. Sumoylation plays important roles in transcription, import/export of proteins from the nucleus, and DNA repair (Hilgarth *et al.*, 2004). Sumoylation can also function to antagonize an ubiquitin site preventing protein degradation (Hilgarth *et al.*, 2004). Neddylation activates cullins, E3 ligases of ubiquitin, leading to ubiquitination and subsequent degradation of negative regulators of cell cycle progression (Liakopoulos *et al.*, 1998). Thus the Nedd8 Ubl acts as an additional layer of control of ubiquitination. Conjugation by Apg12 to Apg5 is required for the formation of vesicles for during autophagy (Mizushima *et al.*, 1998).

Identification and Initial Characterizations of Urm1

Urm1 was first identified in a BLAST search, of the yeast *S. cerevisiae* genome, for sequences related to the *E. coli* protein MoaD (Furukawa *et al.*, 2000). MoaD is a small protein that functions in thiamin biosynthesis and molybdenum biosynthesis (Taylor *et al.*, 1998). MoaD is activated by MoeB, a protein that shares homology with the E1 activating enzymes, to form an acyl-adenylate that can then be converted to a thiocarboxylate allowing it to donate sulfur in biosynthetic pathways (Pitterle *et al.*, 1993). MoaD shares similar fold architecture to the eukaryotic ubiquitin family of proteins, including a conserved glycine-glycine motif.

As is true for other Ubls, Urm1 shares features with ubiquitin and ubiquitin conjugation. First, although sequence similarity of ubiquitin is low (~6% identity), the Urm1 secondary and tertiary structure puts it squarely in the ubiquitin family (Singh *et al.*, 2005). It is interesting to note, however, that Urm1 shows greater sequence similarity to the prokaryotic protein MoaD (~20%) than to eukaryotic Ubls (Singh *et al.*, 2005; Xu *et al.*, 2006). This fact has lead to speculation that Urm1 is the most ancient eukaryotic Ubl and may represent an evolutionary transition for sulfur transfer function to protein conjugation function (Furukawa *et al.*, 2000). Second, the enzymology of Urm1 conjugation to target proteins appears to be similar to the enzymology of ubiquitin conjugation. This conclusion follows for two experimental results: mutation of the C-terminal Urm1 glycine-glycine motif prevents conjugation and an E1 enzyme, Uba4, is required for Urm1 conjugation. Uba4 has clear homology to E1 enzymes that function in the ubiquitin family (Furukawa *et al.*, 2000). However, despite the clear existence of an E1 enzyme for Urm1, as yet no E2 or E3 enzymes have been identified. Urm1 has homologs in all eukaryotic species and this conservation highlights the question: what is Urm1's function in the cell?

Hints to Urm1 function first came from analysis of *urm1Δ* and *uba4Δ* strains in yeast. The deletion of *URM1* or *UBA4* is viable, unlike the deletion of either ubiquitin or sumo. However knocking out the urmylation system disrupts a diverse set of cellular

processes including filamentous growth (FG), tRNA modification, response to oxidative and oleate stress, and TOR dependent nutrient sensing (Huang *et al.*, 2008; Goehring *et al.*, 2003; Lockshon *et al.*, 2007; Rubio-Texeira *et al.*, 2007). It is this diversity of seemingly unrelated cellular functions that is intriguing for the function of Urm1.

The observation that *urm1Δ* mutants are defective for filamentous growth and for TOR pathway signaling, two processes that involve nutrient sensing, suggest that Urm1 may play some role in nutrient sensing. When haploid yeast are starved for nitrogen or carbon, they undergo a morphological and cellular change called filamentous growth. The yeast grow in a defined way to search out nutrients by elongating their cell structure and budding in a distal pattern (Gimeno *et al.*, 1992). Both *urm1Δ* and *uba4Δ* strains fail to elongate, thereby disrupting filamentous growth. Interestingly, the cells do still bud distally (Goehring *et al.*, 2003). The ability of cells to sense nutrient availability is may also be disrupted in *urm1Δ* mutants, evidenced by their sensitivity to rapamycin (Goehring *et al.*, 2003). The drug rapamycin targets a set of kinases, Tor1 and 2, that are responsible for signaling the nutrient status in the cell (Hardwick *et al.*, 1999). The drug activates the kinases causing the cells to behave as though they are deprived of nutrients, regardless of the actual nutrient availability. Activation of the TOR pathway arrests translation and transcription, stopping growth. One facet of TOR signaling involves two transcription factors Nil1 and Gln3 (Rubio-Texeira *et al.*, 2007). These transcription factors are kept in the cytoplasm during normal nutrient levels; however, upon activation of the TOR pathway, the transcription factors are transported to the nucleus (Stanbrough *et al.*, 1995; Beck *et al.*, 1999). In strains lacking Urm1, Gln3 and Nil1 are localized to the nucleus regardless of the nutrient status of the cell (Rubio-Texeira *et al.*, 2007). It also appears that the sensitivity to rapamycin is also related to these transcription factors as loss of Gln3 and Nil1 suppresses *urm1Δ* mutant sensitivity. Unfortunately, the group was unable to identify why loss of Urm1 disrupts Gln3/Nil1 localization.

The understanding of Urm1's function in the cell would be greatly improved by the identification of urmylated conjugates. To identify Urm1 conjugates, the Sprague lab developed a rabbit antibody to Urm1 (Goehring *et al.*, 2003). Western analysis using the

Urm1 antibody reveals a pattern of multiple potentially urmylated conjugates (Figure 1.1). The most prominent band in the western blot has been identified via mass spectrometry as the enzyme, Ahp1 (Goehring *et al.*, 2003). Ahp1, an alkyl hydroxyperoxidase, is important for general response to oxidative stress (Lee *et al.*, 1999). An *ahp1Δ* strain is extremely sensitive to tBOOH (tert-butylhydroperoxide) and hydrogen peroxide, both of which cause a general oxidative stress response but is only slightly sensitive to diamide, which oxidizes gluthatoine. Interestingly, an *urm1Δ* strain is not sensitive to tBOOH or hydrogen peroxide but is sensitive to diamide stress (Goehring *et al.*, 2003). Urm1 appears to be important only in the response to specific types of oxidative stress. The greater sensitivity of a *urm1*Δ mutant to diamide than compared to a *ahp1*Δ mutant may suggest the existence of other urmylated oxidative response enzymes. The identification of Ahp1 as an Urm1 conjugate opens the door for study of mechanics and function of Ahp1's urmylation.

Dissertation Summary

This dissertation encompasses my work to understand the function of Urm1 in *S. cerevisiae*. In chapter II, I use Ahp1 as a model to understand the consequence of urmylation and attempt to identify the site of Urm1 conjugation. In chapter III, I discuss my work to identify new interactions and conjugates of Urm1 through a set of screens in yeast: a synthetic lethal screen, a two-hybrid screen, and a protein over-expression array screen. Finally, in chapter IV, I will discuss work preformed by other groups that assign a role to Urm1 as a sulfur carrier and the impact this has on the hypothesis that Urm1 acts as a post-translational modification.

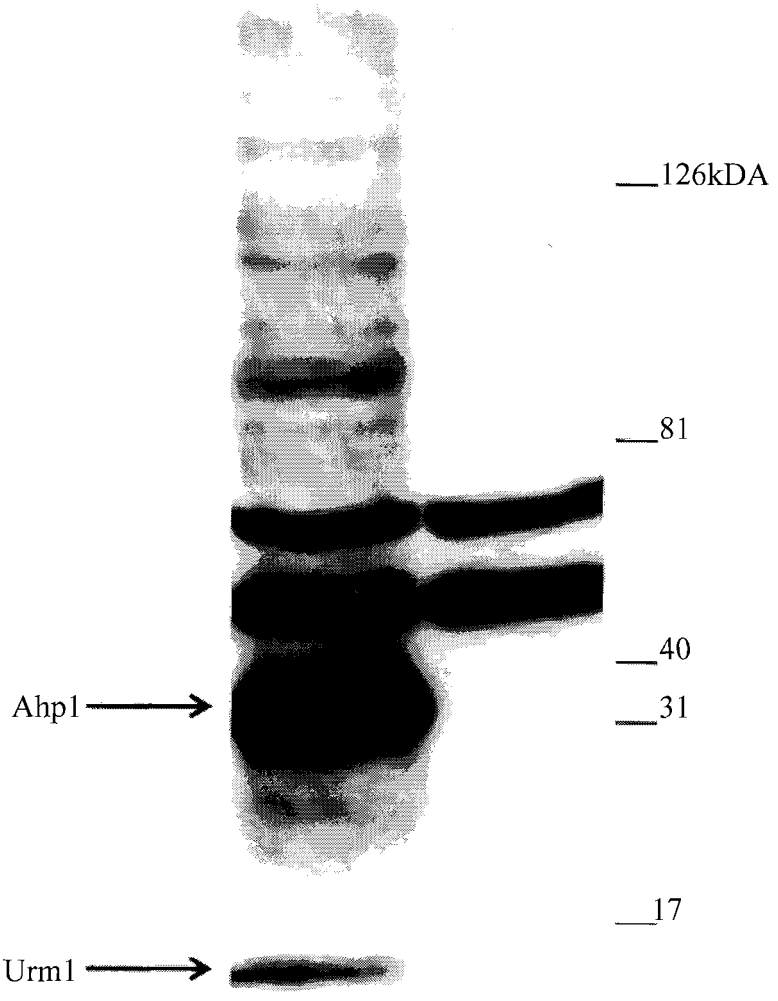

Fig. 1.1. **Western analysis of Urm1 conjugation.** Whole cell extract from strains BY4741 (WT) and SY3839 (*urm1Δ*) examined by western blot analysis. Probed with Urm1 antibodies. Urmylated Ahp1 is 32 kDA.

CHAPTER II

UNDERSTANDING THE ROLE OF AHP1 URMYLATION

Introduction

The discovery that Ahp1 is urmylated opened the door to address questions about the function and mechanism of Urm1. Ahp1 is a small enzymatic protein, about 19kDA. It is a member of a thiol-specific peroxiredoxin family of reductase enzymes, which directly reduces oxidized species, and themselves are recycled by coupling to the thioredoxin system (Lee *et al.*, 1999). Oxidative species can damage DNA, proteins, membrane lipids and upset the general redox state of the cell. In thioredoxin systems, the oxidative species is reduced directly via the oxidation of the catalytic cysteine of the peroxiredoxin, such as Ahp1 (Carmel-Harel *et al.*, 2000). The oxidized Ahp1 then forms a disulfide homodimer, inactivating the enzyme. A thioredoxin reductase, in conjunction with thioredoxins, reduces the Ahp1 disulfide homodimer using NADPH as an electron donor (Prouzet-Mauleon *et al.*, 2001). Disrupting the disulfide reactivates Ahp1 and recycles the enzyme for further use in the response to additional oxidative species.

Ahp1 is specifically involved in repairing damage caused by organic peroxides. Loss of Ahp1 leads to extreme sensitivity to the organic peroxide tert-butylhydroperoxide (tBOOH), which can oxidize lipids. Ahp1 is not required for response to more general oxidative stress, such as exposure to hydrogen peroxide (Lee *et al.*, 1999). An *ahp1Δ* mutant shows moderate sensitivity to the organic peroxide diamide, an oxidative stress that oxidizes thiol species and disrupts the cell's gluthianone system (Lee *et al.*, 1999, Kosower *et al.*, 1987). Ahp1's enzymatic activity can be measured *in vitro.* Ahp1 will reduce tBOOH in the presence of core thioredoxin components: thioredoxin, thioredoxin reductase and NADPH. The conversion of NADPH to NADP can be measured spectrophotometrically to determine Ahp1's activity (Prouzet-Mauleon *et al.*, 2001).

Ahp1 is localized to the cytoplasm but does contain a peroxisomal sorting signal. Ahp1 has never been observed to localize to peroxisomes, however the cells were not subjected to oxidative stress (Lee *et al.*, 1999). In response to a different sort of oxidative stress, respiration of the fatty acid oleate, Ahp1 localizes to the mitochondria but loss of Ahp1 does not cause sensitivity to oleate (Farcasanu *et al.*, 1999).

Ahp1 was the first Urm1 conjugate identified because it is the most abundant species observed in a western blot of whole cell yeast lysate probed with Urm1 antibodies (Figure 1.1). The prominent band was chosen for analysis, cut from the protein gel and subjected to mass spectrometry (Goehring *et al.*, 2003). Several of the predicted peptide sequences matched Ahp1. Confirmation of the existence of an Ahp1-Urm1 conjugate was achieved by two experiments. First, the band at 30kDA isn't seen in western analysis of crude lysates from an *ahp1Δ* null mutant. Second, when Ahp1 is tagged with GST and immunoprecipitated, an Ahp1-GST species is detected in a Urm1 western blot. In support of a role for Urm1 conjugation in response to oxidative stress, *urm1Δ* mutants are sensitive to diamide (Goehring *et al.*, 2003). It is important to note however, that *urm1Δ* mutants are more sensitive to diamide than are *ahp1Δ* mutant cells, suggesting there may be other Urm1 conjugates related to response to diamide (Figure 2.1). Urm1's role in oxidative stress appears specific to diamide, as *urm1Δ* mutants are not sensitive to tBOOH.

Armed with a target of Urm1 conjugation, Ahp1, questions about the mechanics of Ahp1's conjugation and cellular outcome of conjugation for Ahp1 may be addressed.

Identifying the Site of Urmylation

In the ubiquitin system, ubiquitin is conjugated to the lysines of target proteins. Other ubiquitin-like systems also follow this path of conjugation making it a reasonable hypothesis that Urm1 is also conjugated to targets via lysine residues. Therefore, there may be a particular lysine on Ahp1 that is urmylated. With the site of urmylation identified, I could then test changes to Ahp1's function in a precise way that removes unintended consequences of examining null mutants. In other ubiquitin-like systems,

specific lysines are flanked by consensus sequences, facilitating identification of the site by the conjugation machinery. Identification of the site of conjugation of Urm1 to Ahp1 may help identify a consensus motif of urmylation. Once other urmylation targets are known an urmylation motif will facilitate the search for new urmylation targets and proteins that may recognize this motif.

The fact that Ahp1 and Urm1 are conserved throughout eukaryotes prompted me to search for the sites of urmylation at conserved lysines within Ahp1. Fortunately, due to its size, Ahp1 has only thirteen lysines, five of which are strongly conserved (Figure 2.2). Initially, five single mutants were created at each of these lysines using site-directed mutagenesis. Each conserved lysine was mutated to an arginine, maintaining the charge of the protein but preventing conjugation of Urm1 (Table2.1).

Table 2.1. **Ahp1, lysine to arginine mutant plasmids**. Ahp1 was cloned into the pRS303 vector. Lysine to arginine changes were achieved via PCR driven site directed mutagenesis. **RED**: highly conserved lysine, **GREEN**: moderately conserved.

Plasmid	K to R change	# of changes
Empty	pRS303	0
WT	Wild Type Ahp1	0
47	47	1
48	48	1
79	79	1
81	81	1
102	102	1
5R	47, 48, 79, 81, 102	5
6R	32, 47, 48, 79, 81, 102	6
7R	32, 41, 47, 48, 79, 81, 102	7
9R	32, 41, 47, 48, 79, 81, 102, 113, 124	9
10R	32, 41, 47, 48, 79, 81, 102, 113, 124, 156	10

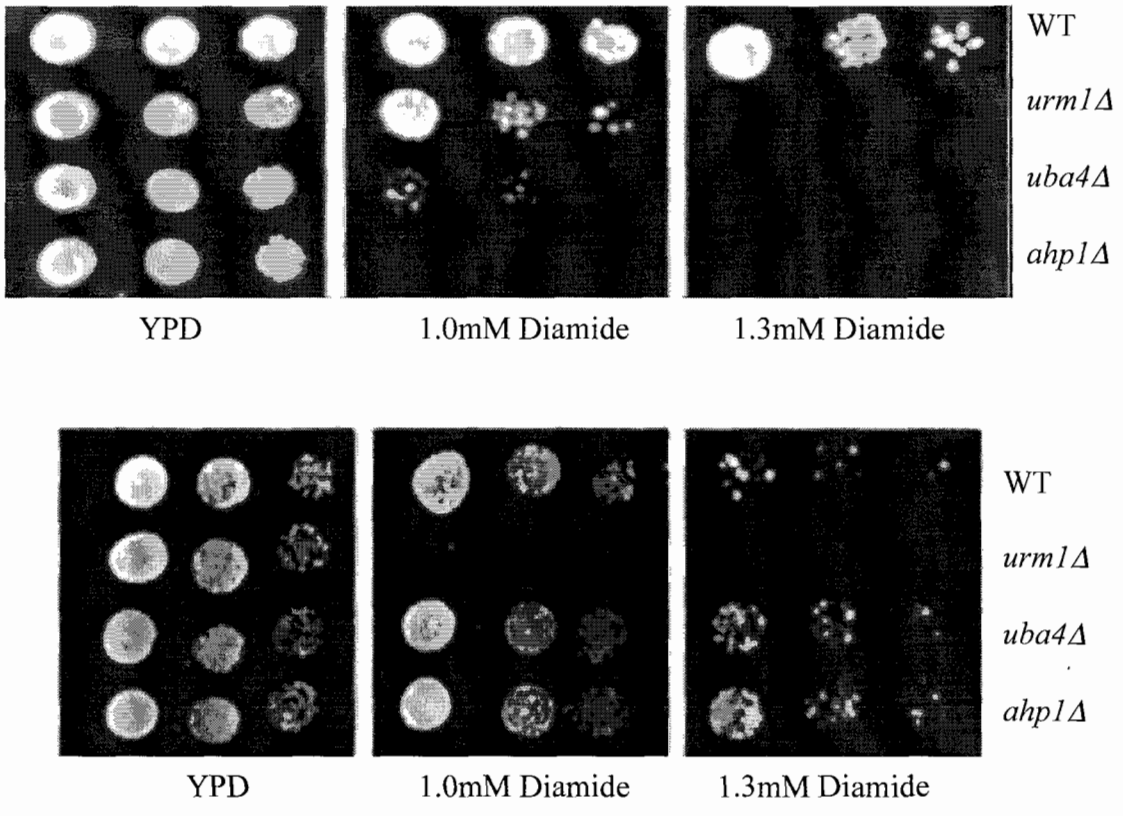

Fig. 2.1. **Sensitivity of *ahp1Δ*, *urm1Δ*, and *uba4Δ* mutants to tBOOH and diamide.** Serial dilutions of BY4741 (WT), SY4119 (*ahp1Δ*), SY3839 (*urm1Δ*), SY3840 (*uba4Δ*). Strains where plated at 0.7 OD_{600} and serially diluted at 1/10 ratios. Incubated for three days at 30°C.

Expression of each Ahp1 mutant is driven by the constitutive promoter *ADH1* in the pRS303 plasmid vector. The mutants were transformed into an *ahp1Δ* background and tested for their ability to restore drug resistance (Figure 2.3 A). Each single lysine mutant change restored drug response, indicating that enzymatic function of Ahp1 was still intact. The status of Ahp1 urmylation was then examined by western blot using an Urm1 antibody (Figure 2.4 A). None of the single conserved lysine mutant changes abolished urmylation of Ahp1.

Ubiquitin systems tend to exhibit conjugation of the Ubl to a preferential lysine site, but it is not uncommon for machinery to conjugate to other lysines if the preferred site is removed (Personal communication, Biggins laboratory). In an attempt to eliminate this possibility, I created multiple lysine-to-arginine mutants, beginning with a mutant lacking all five conserved lysines. The quintuple mutant restored drug resistance, suggesting it had not lost all of Ahp1's activity. However, this mutant was still urmylated (Figure 2.4 B). I then further mutated Ahp1, creating lysine to arginine mutants at eight and ten sites (Table 2.1). The stability and function of Ahp1 in the eight- and ten-change mutants is in doubt as they failed to restore drug resistance (Figure 2.3 B).

MSDLVN**KK**FPAGDY**K**FQYIAISQSDADSESC**K**MPQTVEWS**K**LISEN**KK**WIITGA
PAAFSPTCTVSHIPGYINYLDEL**V**K**E**KEVDQWIVVTVDNPFANQAWA**K**SLGV**K**D
TTHI**K**FASDPGCAFT**K**SIGFELAVGDGVYWSGRWAMVVENGIVTYAA**K**ETNPG
TDVTVSSVESVLAHL

Fig. 2.2. **Conserved lysines of Ahp1.** The protein sequence of Ahp1 was aligned using ClustalW (Thompson *et al.*, 2002). Five lysines are highly conserved (**RED**), five are moderately conserved (**GREEN**), and four are poorly conserved (**BLUE**).

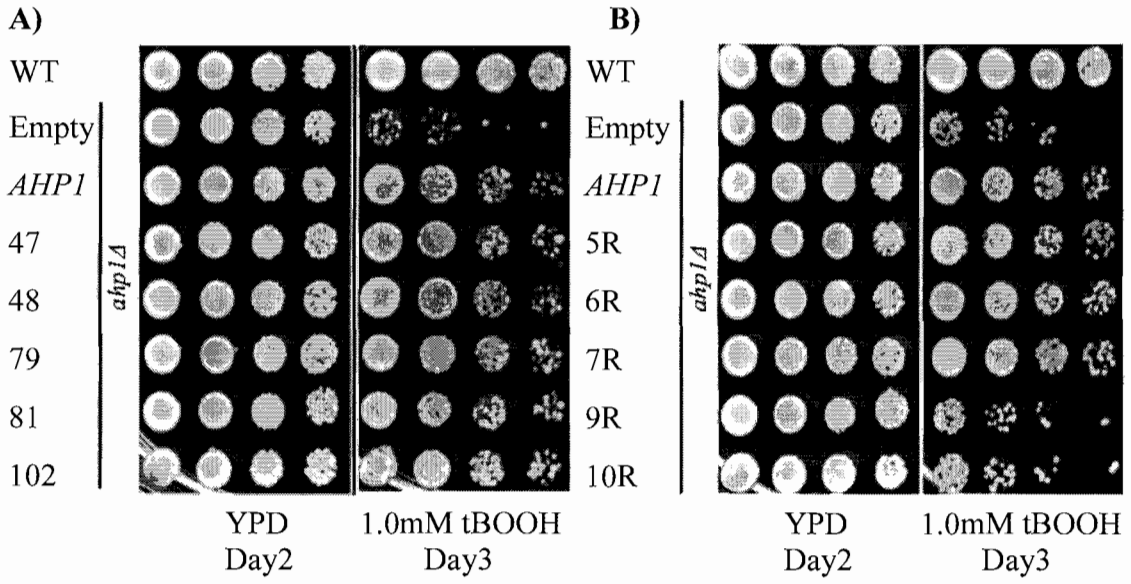

Fig. 2.3. **Response of Ahp1 mutants to tBOOH stress**. Serial dilutions of BY4741 (WT) + pRS303 and SY4119 (*ahp1Δ*) transformants (Table 2.1). Cells were plated at 1.0 OD_{600} and serially diluted at 1/5 ratios. **A)** Single lysine to arginine change mutants. **B)** Multiple lysine to arginine change mutants.

However, even the eight- and ten-change mutants were still urmylated, although the urmylated Ahp1 band was weak, perhaps due to the protein's instability (Figure 2.4 B).

Given the failure to disrupt Ahp1 urmylation in a ten-lysine-to-arginine change mutant, I changed my strategy for identifying the site of urmylation. There are several possibilities why I failed to identify the target lysine. First it is possible that the urmylation machinery is imprecise, conjugating any free lysine. Second, I may have missed the target lysine, it may not be conserved. Third, it is possible that conjugation does not occur on a lysine at all. To address the fundamental problems of identifying the site of conjugation through mutagenesis, I sought to purify urmylated Ahp1 and identify the conjugation site via of mass spectrometry analysis.

The purification of Urmylated Ahp1

Obtaining purified urmylated Ahp1 would allow me to ask several fundamental questions about the function of urmylation and the mechanism of conjugation. The

purified urmylated Ahp1 could be analyzed by mass spectrometry to determine the site or sites of urmylation. Further, mass spectrometry analysis will also allow me to confirm if urmylation behaves like other ubiquitin-like systems, where an isopeptide bond conjugates the glycine of Urm1 to the lysine of Ahp1. Determining the affect of urmylation on Ahp1's enzymatic activity also requires purification of the urmylated species. Purified Urm1-Ahp1 in hand, I could then test Ahp1's ability to reduce oxidative species *in vitro*, following the consumption of NADPH spectrophotometrically.

To isolate the Urm1-Ahp1 species, I chose to immunoprecipitate it from a yeast lysate produced from cells over-expressing Urm1 via a plasmid-borne tetracycline promoter. The predominant urmylated species is Ahp1 (Figure 1.1) and Ahp1 itself is expressed at fairly high levels in the cell (Huh *et al.*, 2003). A Urm1 antibody functions poorly for the purposes of immunoprecipitation, as its conjugation to sepharose beads significantly reduced its ability to recognize Urm1. I therefore turned to tagging Ahp1 with several commercial motifs to use for immunoprecipitation. I examined several C-terminally tagged chromosome versions of Ahp1 including GFP and GST for three qualities: activity of Ahp1 as indicated by drug resistance, detection of the tagged protein by antibodies to the tags, and immunoprecipitation of the tagged protein. Both tagged constructs exhibited at least partial Ahp1 function (Figure 2.5 C). Ahp1-GFP immunoprecipitated very poorly (data not shown). Both GST and Urm1 antibodies detected GST-tagged Ahp1 robustly in a western blot (Figure 2.5 A,B), but I was never able to observe the urmylated Ahp1 species with GST antibodies in the whole cell extract. Although I could not detect urmylated tagged Ahp1 with GST or GFP antibodies, I could detect urmylated Ahp1 with Urm1 antibodies; the Urm1-Ahp1 band increased to the predicted size for adding a GST (Figure 2.5 A,B).

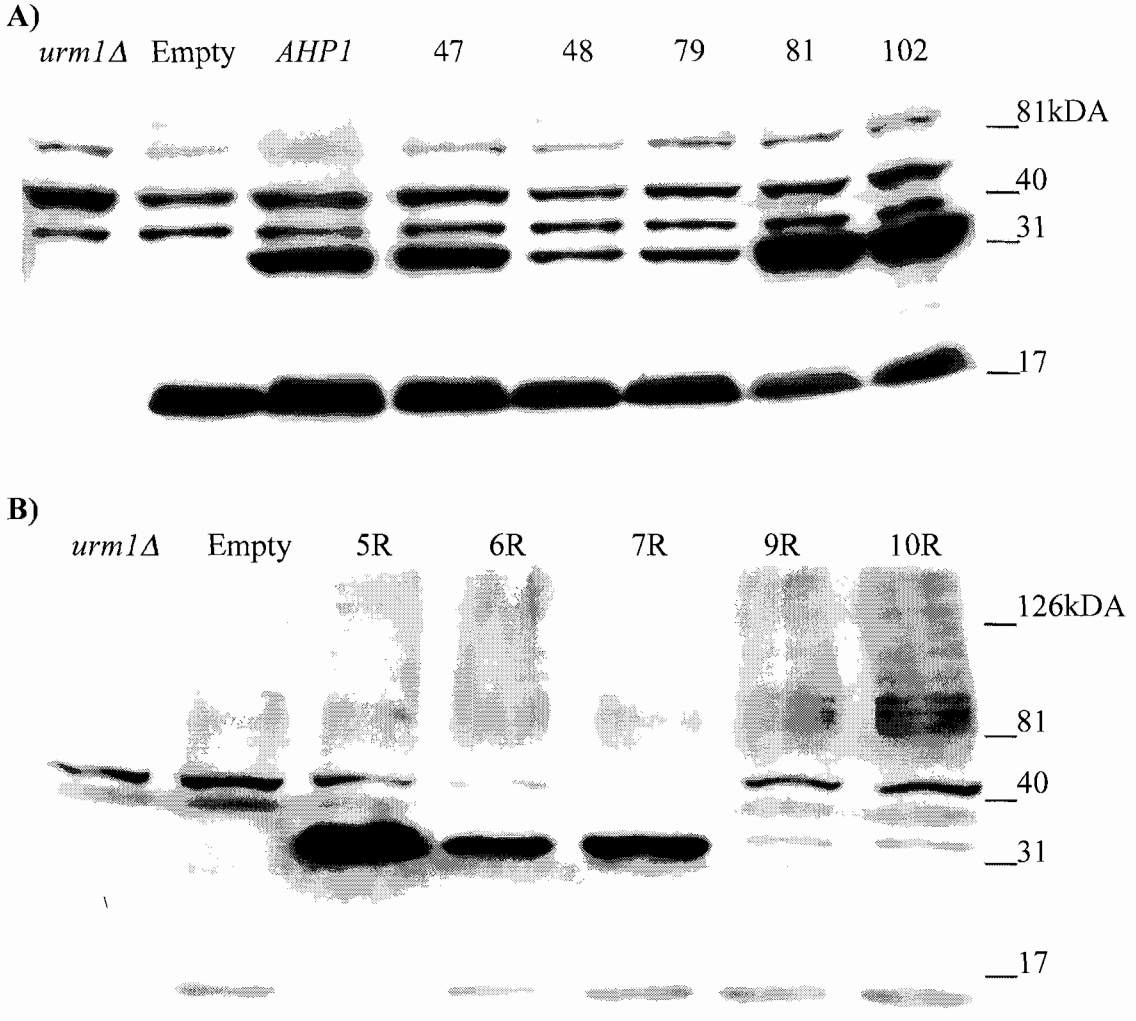

Fig. 2.4. **Urmylation of Ahp1 lysine to arginine mutants.** SY4119 *(ahp1Δ)* expressing Ahp1 plasmids (Table 2.1). Whole cell extracts were isolated from transformants during mid-log growth. Western blots of extracts was probed with Urm1 antibodies. None of the Ahp1 mutants eliminated urmylation. Urmylated Ahp1 is 32kDa in size. **A)** Single lysine to arginine mutants. **B)** Multiple lysine to arginine mutants.

The failure to detect urmylated tagged Ahp1 with the GST or GFP antibody, even though it could be detected with the Urm1 antibody, suggested that the Urm1 antibody was more sensitive than either GST or GFP antibody. To address this possibility and to assess the amount of urmylated Ahp1-GST that could be isolated, I scaled the GST immunoprecipitation up to 100ml of cell culture and concentrated the GST elute in a protein size exclusion centrifuge column in the attempt to obtain enough urmylated Ahp1 to be detected by the GST antibody (Figure 2.6). To estimate the ratio of urmylated GST-Ahp1 to free GST-Ahp1 I loaded a known amount of GST-Urm1. Comparing the concentrated GST-Ahp1 elutes to the known GST-Urm1 standard it was clear that very little urmylated Ahp1 was present, less than 0.1ng of protein. The GST blot indicates that approximately 10-20ng of GST-Ahp1 was isolated, based on comparison to GST-Urm1. Thus I conclude that only about 0.5-1.0% of the pool of Ahp1 is urmylated, even when Urm1 is over-expressed. It is also follows that the GST antibody was unable to detect the urmylated GST-AHP1 because of the low abundance of urmylated GST-Ahp1; the GST-antibody required at least 1ng of protein for detection (Figure 2.6). The low yield of urmylated Ahp1 prevented moving forward with the mass spectrometry project to determine the site of urmylation or with *in vitro* characterization of Ahp1's activity.

There are several possible explanations for the low population of urmylated Ahp1. The conjugation of Ahp1 may be transient. For instance, urmylation could be part of a recycling pathway; once reduced, Ahp1's Urm1 conjugation may be removed. Another possibility is that urmylation of Ahp1 may be important only during specific environmental conditions and only during those periods is there a large pool of urmylated Ahp1. Lastly, to date a de-urmylating enzyme has not been identified. Ubiquitin and many of the ubiquitin-like systems have isopeptidases that remove ubiquitin from conjugated targets. If a de-urmylating enzyme exists, it may keep the pool of urmylated Ahp1 low. The presence of this isopeptidase may antagonize efforts to isolate urmylated Ahp1.

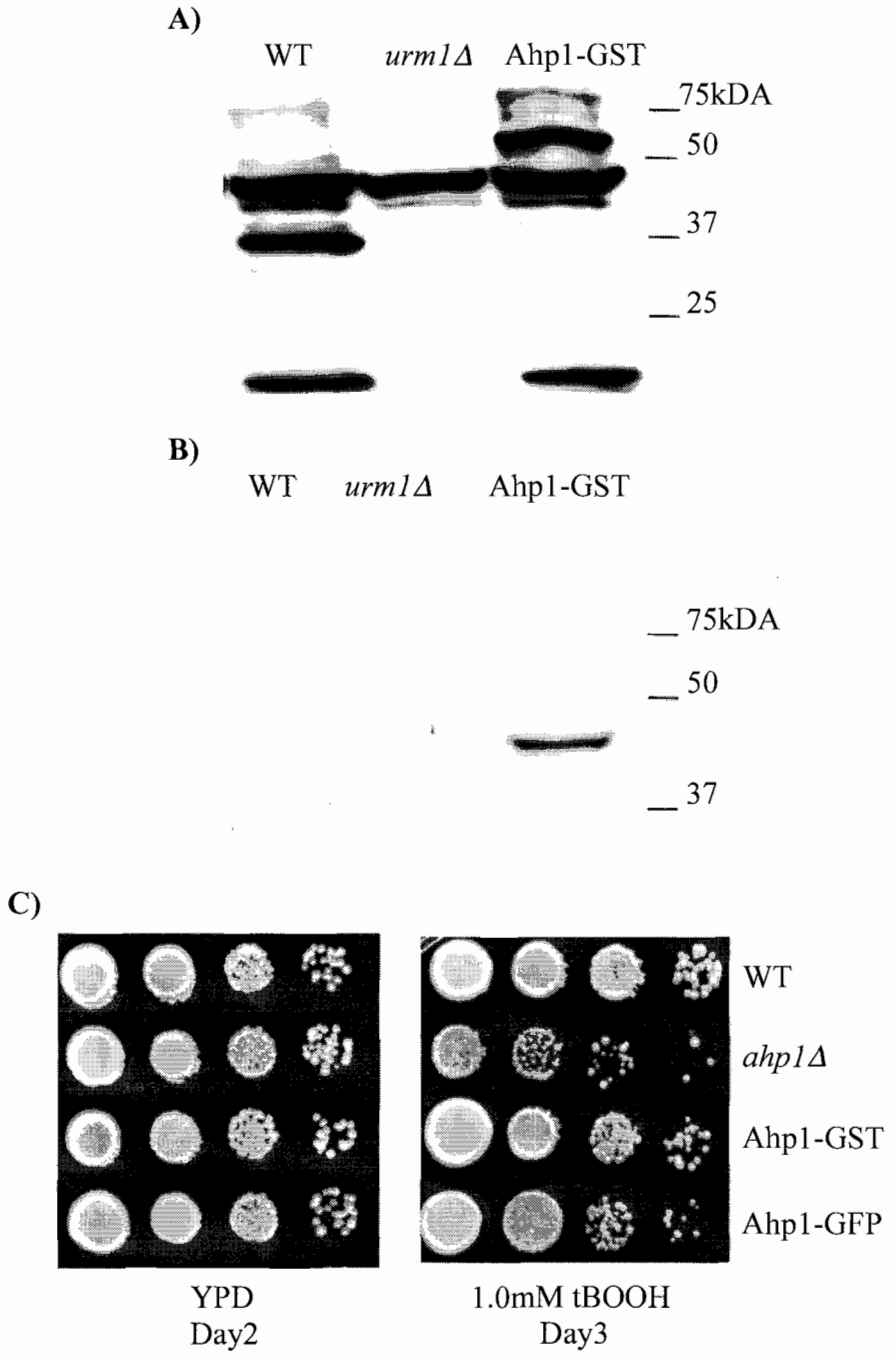

Fig. 2.5. **Tagging Ahp1 with the epitope GST**. Ahp1 was C-terminally chromosomally tagged with GST, SY4319 or GFP, SY4291. **A)** & **B)** Whole cell extract from strains BY4741 (WT), SY3839 (*urm1Δ*), and Ahp1-GST was examined by western blot. Urmylated Ahp1 is 32 kDA, Urmylated Ahp1-GST 55kDA, Ahp1-GST 44kDA. **A)** Probed with Urm1 antibodies. **B)** Probed with GST antibodies. **C)** Cells were plated at 1.0 OD_{600} and serially diluted at 1/5 ratios.

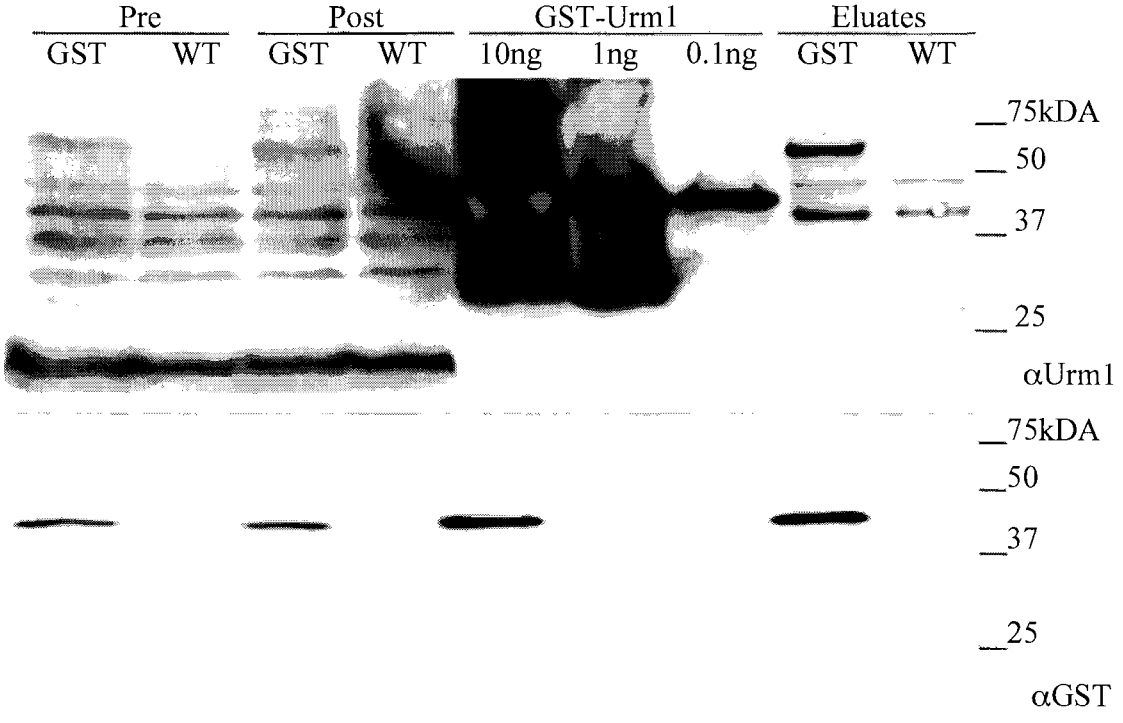

Fig. 2.6. **Native immunoprecipitation of urmylated GST tagged Ahp1**. Lysates from SY4319 (Ahp1-GST) and BY4741 (WT), expressing CY3937 (URM1), were immunoprecipitated using glutathione beads. Pre: Lysates before binding to beads, 1% loaded. Post: Lysate after binding to beads 1% loaded, Eluate: after concentration 30% loaded. GST-Urm1 was isolated in E. coli and quantified by Bradford assay. Ahp1-GST is 44kDA, urmylated 55kDA.

The Dependence of Ahp1's Localization on Urm1

Posttranslational modification by ubiquitin-like molecules can act as a signal for localization. For instance, Sumo can act as a signal for transport to the nucleus (Hilgarth *et al.*, 2004). Ahp1 is cytoplasmic during normal growth conditions and will localize to the mitochondria during oleate respiration (Farcasanu *et al.*, 1999). Ahp1 also has a predicted peroxisomal localization signaling motif, but as stated above there is no literature that reports Ahp1 localizing to the peroxisomes (Lee *et al.*, 1999). Using a chromosomally tagged Ahp1-GFP construct, I examined the localization of Ahp1 in the presence and absence of Urm1 during exponential growth and following exposure to diamide or oleate. During exponential growth and following exposure to diamide, Ahp1 was localized to the cytoplasm both in the presence or absence of Urm1 (Figure 2.7 A,B). As published previously, Ahp1 localized to the mitochondrion during oleate respiration but the loss of Urm1 did not have an effect on this localization (Figure 2.8). I was not able to examine the affect of tBOOH on Ahp1 localization because exposure to tBOOH quenched the GFP signal (data not shown). Under the conditions I examined, Ahp1's localization does not depend on the presence of Urm1.

Conclusion

The use of Ahp1 as a model for urmylation has reached a technical limit due to the low quantities of urmylated Ahp1 in the cell. Based on my immunoprecipitation data only 0.5-1% of Ahp1 is urmylated during exponential growth, even in cells over-expressing Urm1. If Ahp1 is the predominant urmylated band on an Urm1 western blot of cell lysate then the levels of all urmylated proteins must be very low. Several factors could explain the low levels of urmylation: transient conjugation, conditional conjugation, and the action of a de-urmylating enzyme. Without sufficient purified urmylated Ahp1 I am unable to determine the sites of conjugation by mass spectrometry or investigate whether urmylation causes a change to enzymatic activity. I was also unable to observe an affect of urmylation on Ahp1 localization. The function of urmylation of Ahp1 is still unclear.

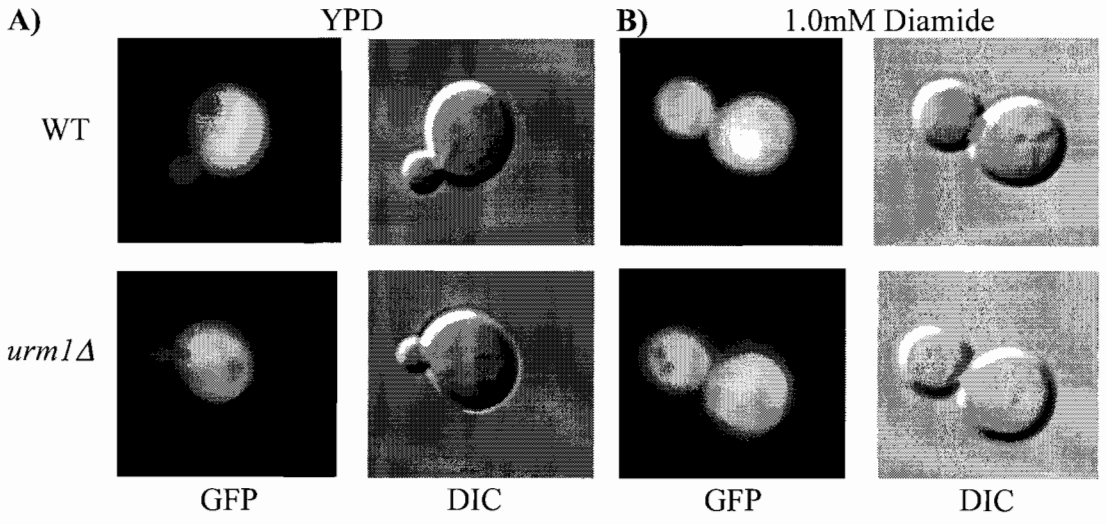

Fig. 2.7. **The localization of Ahp1 in YPD and 1.0mM diamide.** SY4291 (WT/Ahp1-GFP) and SY4292 (*urm1Δ*/Ahp1-GFP) were grown to mid-log in liquid YPD media. Ahp1-GFP was visualized with a GFP fluorescence filter and DIC. A) Cells from YPD media. B) 1.0mM Diamide was added to mid-logged YPD cultures for 20 minutes.

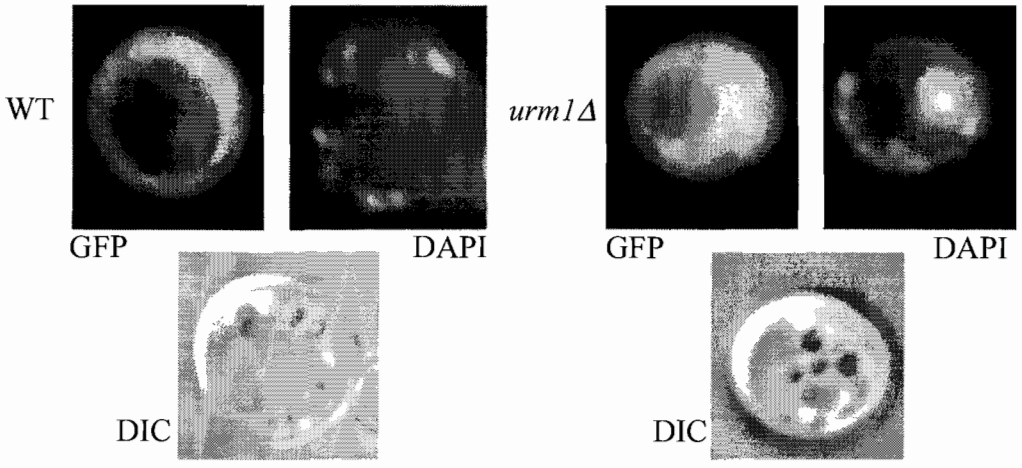

Fig. 2.8. **The localization of Ahp1 during Oleate growth conditions.** SY4291 (WT/Ahp1-GFP) and SY4292 (*urm1Δ*/Ahp1-GFP) in 0.2% Oleate media were examined under the microscope under the GFP fluorescence filter, DIC, and UV filter for DAPI visualization to identify mitochondria.

CHAPTER III

SCREENING *S. CEREVISIAE* FOR URM1 INTERACTIONS AND CONJUGATES

Introduction

In early 2007, very little was known about Urm1. Only one conjugate had been identified, Ahp1, and the consequence of its urmylation remained unclear (Goehring *et al.*, 2003). Hints to the importance of Urm1's function were found in the phenotypes of an *urm1*Δ mutant: disruption of filamentous growth and sensitivity to the two drugs, rapamycin and diamide (Goehring *et al.*, 2003). However, these phenotypes provide no explanation for how these cellular responses are dependent on Urm1 function. Taking advantage of *S. cerevisiae's* genetic versatility and the array tools that enable screening for phenotypes of interactions on a genome-wide scale, I set out to perform a series of screens: a synthetic lethal screen, a two-hybrid screen, and a protein over-expression array screen. A synthetic lethal screen examines the fitness of strains carrying two non-lethal null mutations (Tong *et al.*, 2001). If the double mutant is lethal or sick, there may be a relationship between the same cellular processes controlled by the two genes. A two-hybrid screen detects physical interactions between proteins by following reporters whose transcription is dependent on the transcription factor domains fused to the proteins (Fields *et al.*, 1989). The two-hybrid screen provides the opportunity to identify Urm1 conjugates, urmylation machinery, and proteins that have Urm1 binding domains. The last screen uses an ordered array that permits examination of the consequence of the over-expression of each gene (Sopko *et al.*, 2006). In my work I have used the over-expression array to investigate sensitivity to diamide. The over-expression of a negative regulator of urmylation may mimic an *urm1Δ* strain and confer sensitivity to diamide. A gene that encodes an enzyme that de-urmylates proteins might be such a negative regulator.

Concurrent with my work, a technician in our lab, Kim Landreth, preformed a mass spectrometry screen of Urm1 immunoprecipitates to identify Urm1 conjugates.

Screening for Synthetic Lethal Genetic Interactions Via SGA

SGA (synthetic genetic analysis) uses an array comprised of single null yeast mutants of each non-essential gene, developed by the Boone Lab (Tong *et al.*, 2006). The array is designed such that a query strain, with a desired mutation, can be mated to each knockout strain in the array. Through a selection process driven by marked genes whose expression demands the haploid state and by marked null mutations, a library of haploid double null mutants is created (Figure 3.1). Using SGA, I was able to perform a synthetic lethal screen using an *urm1Δ* mutant as my query gene to determine which *urm1Δ yfgΔ* (Your Favorite Gene) mutants exhibit reduced viability. The synthetic lethal screen provides genetic information that may indicate common dependent cellular pathways. Loss of one gene does not disrupt a cellular process enough to cause a fitness defect; there may be redundant pathways that can compensate for the null mutant, or the pathway may be reduced in efficiency but that reduction is undetectable. In the synthetic lethal screen, loss of two genes in a critical pathway may reduce pathway efficiency sufficiently to produce a phenotype, thereby suggesting a genetic relationship between the two genes. A synthetic lethal screen can also identify double mutants that reduce efficiency in two separate cellular processes that in combination cause a defect in fitness.

The SGA analysis was conducted three times using *urm1Δ* as the query strain (Figure 3.2 A). Mutants that displayed a growth defect on synthetic medium were retested individually (Figure 3.2 B). Twenty-three genes were identified as synthetic sick (thirteen) or lethal (ten) in the *urm1Δ* mutant background (Table 3.1). Disruption of two major cellular processes, transcriptional related events and protein trafficking, make up the majority of synthetic hits. Most of the hits do not group together in known interactive complexes or pathways and are likely to represent global fitness defects due to the addition of the *urm1Δ* mutant, with the exception of the Elongator complex set of genes discussed below.

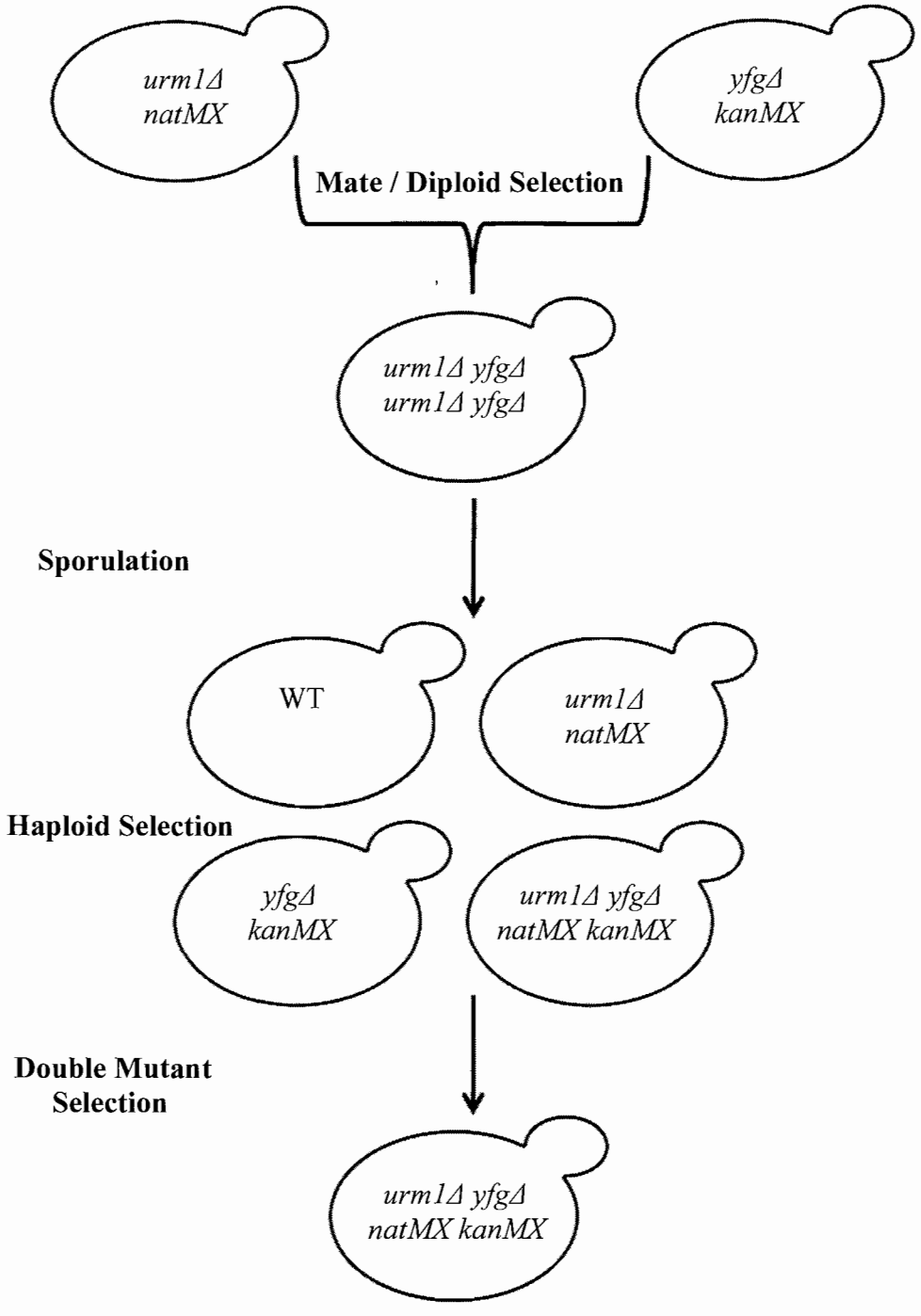

Fig. 3.1. **The SGA protocol.** The query gene is mated into the yeast deletion collection array creating diploids. Diploids were sporulated. After several rounds of haploid selection the double mutants are selected. Protocol is further described in the Materials and Methods section.

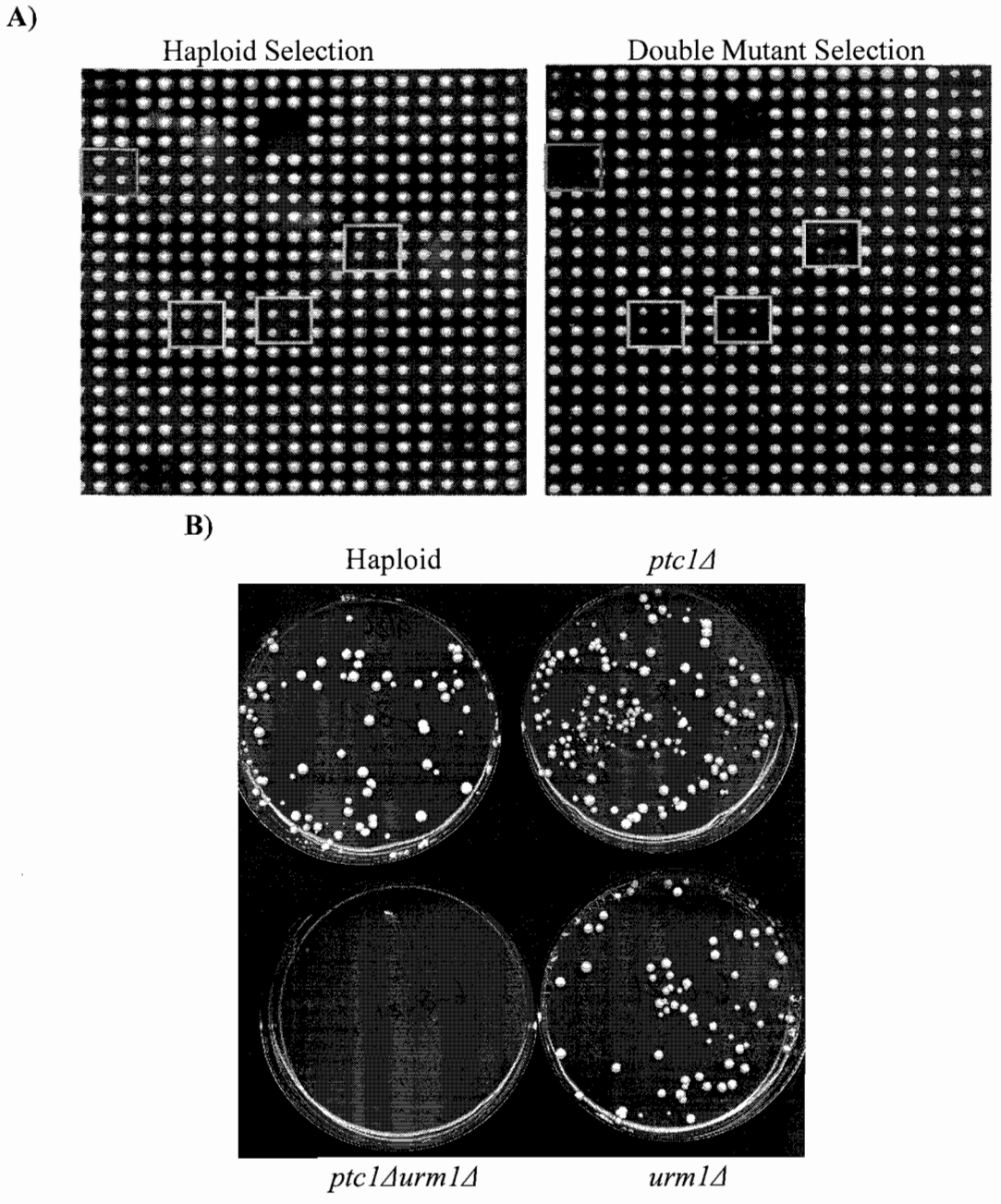

Fig. 3.2. **The synthetic lethal screen of *urm1Δ*.** SY4230 (*urm1Δ*) was mated into a yeast deletion collection following the SGA protocol (Tong *et al.*, 2006). **A)** An example of an SGA *urm1Δ* plate. A reduction in fitness was determined by comparing the haploid selection plate to the plate selecting for the double mutants. RED box is an example synthetic lethal, GREEN box are synthetic sick. **B)** Example of conforming the synthetic phenotype, *ptc1Δurm1Δ*. Each selection plate contains an equal level of cells, described further in Materials and Methods section. The plates select for the phenotype listed.

Table 3.1. **Synthetic genetic interactions of *urm1Δ*.** Synthetic lethal interactions obtained by the SGA protocol. The screen was preformed three times. Gene descriptions were obtained from the Saccharomyces Genome Database, SGD. Color denotes general cellular function: **Transcription,** Cell Organization, **Actin,** Mitochondria, Degradation, Transportation, Unknown.

GENE	Fitness	Description
TEF2	Sick	Translational elongation factor EF-1 alpha.
SGN1	Sick	Cytoplasmic RNA-binding protein.
MPH1	Sick	Member of the DEAH family of helicases, functions in an error-free DNA damage bypass pathway.
ELP1	Lethal	Subunit of Elongator complex.
ELP2	Lethal	Subunit of Elongator complex.
ELP3	Lethal	Subunit of Elongator complex.
ELP4	Lethal	Subunit of Elongator complex.
ELP6	Lethal	Subunit of Elongator complex.
BEM1	Sick	Functions as a scaffold protein for complexes that include Cdc24, Ste5, Ste20.
PTC1	Sick	Phosphatase, inactivates Hog1 in the osmosensing MAPK cascade.
TPM1	Lethal	Tropomyosin; binds to and stabilizes actin cables and filaments.
MAM33	Lethal	Protein of the mitochondrial matrix involved in oxidative phosphorylation.
RIM20	Sick	Involved in proteolytic activation of Rim101, interacts with the ESCRT-III subunits Snf7.
NAS2	Lethal	Protein with similarity to the p27 subunit of mammalian proteasome modulator.
RDM7	Lethal	Subunit of the GET complex.
EPS1	Sick	Pdi1 (protein disulfide isomerase)-related protein involved in endoplasmic reticulum retention of resident ER proteins.
VPS51	Sick	Component of the GARP (Golgi-associated retrograde protein) complex.
BTS1	Lethal	Geranylgeranyl diphosphate synthase, may regulate GTP-binding proteins that mediate vesicular traffic.
MON1	Sick	Peripheral membrane protein with a role in endocytosis and vacuole integrity.
SAC1	Lethal	Lipid phosphoinositide phosphatase of the ER and Golgi, involved in protein trafficking and secretion.

Table 3.1 (continued).

GENE	Fitness	Description
GOS1	Sick	v-SNARE protein involved in Golgi transport.
UBP3	Sick	Ubiquitin-specific protease transport between endoplasmic reticulum and Golgi compartments
DFG10	Sick	Unknown function, involved in filamentous growth.
YIR007W	Sick	Putative protein of unknown function.

The Elongator complex, comprised of six proteins Elp1-6, was initially proposed to drive transcriptional elongation because it was found to interact with the elongating form of the RNA polymerase (Otero *et al.*, 1999). The complex can exist as two discrete subcomplexs. Elp1-3 comprises the core-elongator and Elp4-6 the HAP complex (Winkler *et al.*, 2001). The exact function of each Elongator protein in the complex is not entirely clear. Elp1 is a scaffold protein facilitating the formation of the core complex (Frohloff *et al.*, 2003). Elp3 contains a HAT (histone transferase domain) and is thought to be the major catalytic component of the complex (Wittschieben *et al.*, 1999). Elongator complex has also been ascribed two functions distinct from its role in transcription: exocytosis and tRNA modification (Rahl *et al.*, 2005; Huang *et al.*, 2005; Krogan *et al.*, 2001). One component of the Elongator complex, Elp1, physically interacts with and is required for the transport of Sec2 to the membrane (Rahl *et al.*, 2005). Certain tRNA modifications are dependent on the presence of each component of the Elongator complex (Huang *et al.*, 2005, Krogan *et al.*, 2001). I will discuss the Elongator complex in more detail in Chapter IV.

PTC1, one of the genes identified in the screen, encodes a Ser/Thr phosphatase, and is of particular interest due to its proposed role as a negative regulator of Hog1, a MAPK kinase that functions in the osmosensing pathway (Warmka *et al.*, 2001). In yeast there are several MAPK pathways, three of which share many of the same pathway components: the mating pathway, the filamentous growth pathway and the osomosensing pathway (Gustin *et al.*, 1998). Constitutive activation of Hog1 is lethal (Maeda *et al.*,

1995). If Urm1 is a negative regulator of Hog1, loss of both Urm1 and Ptc1 may lead to lethality. The elucidation of a defined role for Urm1 in signaling in the Hog1 pathway could suggest possibilities for the role of Urm1 in the filamentous growth pathway. In particular, because MAPK signaling cascades share components, it is plausible that a Urm1 role in signaling in the osmosensing pathway could also be repeated in the filamentous growth MAPK signaling cascade. In any event, I will discuss the relationship of Urm1 and Ptc1 on the regulation of Hog1 in Chapter IV.

Identifying Urm1 Interactions Via a Two-Hybrid Screen

A two-hybrid screen is designed to identify potential physical interactions between two proteins. The bait protein is fused to the DNA binding region of a transcription factor, and a query protein is fused to a transcriptional activator domain (Fields *et al.,* 1989). If the bait and query proteins interact physically or through a complex, the transcription factor may become functional and able to activate a set of reporter genes (Fields *et al.,* 1989). Three plasmid libraries comprising the yeast genome tagged with the Gal4 activation domain (AD) can be used to screen the yeast proteome for interactions to a bait protein tagged with the Gal4 DNA binding domain (BD) (James *et al.,* 1996). The strain used to screen the library has three reporters driven by the *GAL4* promoter: *HIS3*, *ADE3,* and *lacZ* (James *et al.*, 1996). The use of three reporters helps eliminate false positives.

To screen the AD libraries for two-hybrid interactions with Urm1, two bait plasmid vectors were created, Gal4BD-Urm1 and Urm1-Gal4BD. Urm1 exists in at least two states in the cell, conjugated and un-conjugated. The N-terminal Gal4BD-Urm1 does not block the glycine-glycine conjugation motif of Urm1 and the construct will likely behave as native Urm1 does. The C-terminal Urm1-Gal4BD construct will prevent conjugation but can potentially mimic the conjugated state, thus increasing the chance of interaction with proteins that interact only with conjugated Urm1. Both Urm1 bait constructs were tested for function by examining sensitivity to drugs (diamide and rapamycin) in an *urm1Δ* mutant (Figure 3.3 A). Gal4BD-Urm1 did restore resistance to

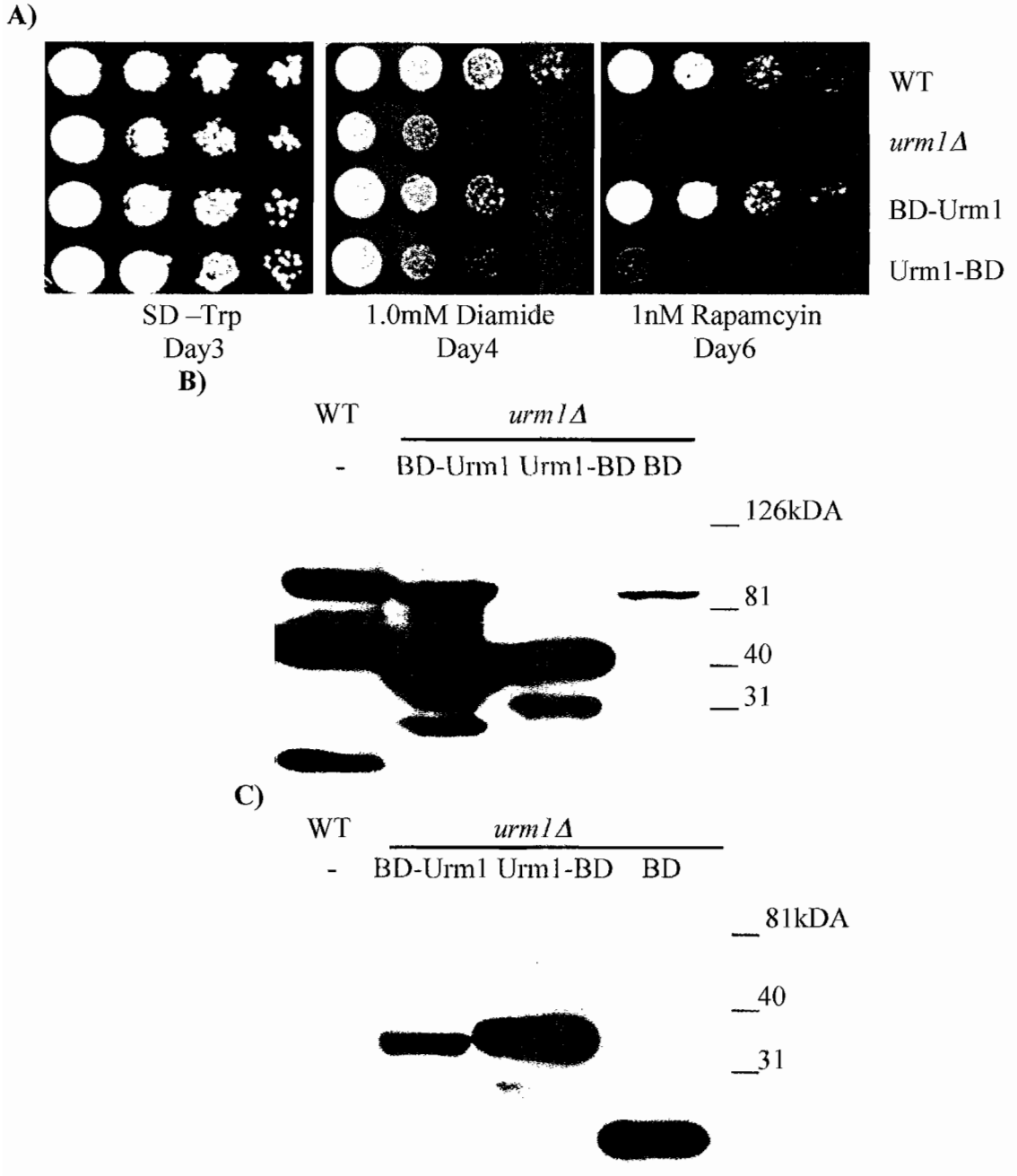

Fig. 3.3. **Testing the fidelity of the Gal4BD-Urm1 and Urm1-Gal4BD.** pCDBD2 (BD), CY3925 (Urm1-Gal4BD) and CY3950 (Gal4BD-Urm1). **A)** BY4741 (WT) + (BD) and SY3839 (*urm1Δ*) + each plasmid were plated at 0.7 OD_{600} and serially diluted at 1/10 ratios. **B) & C)** Whole cell examined by western blot analysis. – harbors no plasmid. BD is 25kDA, Urm1 constructs are 36kDA **B)** Probed with Urm1 antibody **C)** Probed with Gal4BD antibody.

the drugs and as expected the Urm1-Gal4BD did not, due to its inability to conjugate. Expression of the bait vectors was examined by western blots (Figure 3.3 B). Both Urm1 bait proteins were detected by Urm1 and Gal4BD antibodies.

Because detection of two-hybrid interactions is dependent on transcriptional reporters, it was critical to insure that the bait vectors do not activate reporters in the absence of Gal4AD constructs (Figure 3.4). In fact, neither BD construct activated any of the reporters. A two-hybrid interaction between Gal4BD-Urm1 and Gal4AD-Uba4 has been published so I used that interaction as a positive control to test for the activation of the reporters (Figure 3.4) (Furukawa *et al.,* 2000). Gal4BD-Urm1 activated all three reporters in conjunction with Gal4AD-Uba4 as expected. Interestingly, Urm1-Gal4BD only activated the *HIS3* reporter in the presence of Gal4AD-Uba4. The *HIS3* reporter is the most sensitive of the three; it is also the most likely to display false positives (James *et al.,* 1996). If Uba4 does not bind to conjugated Urm1 as readily as to free Urm1 the two-hybrid interaction may only be strong enough to activate the *HIS3* reporter. This outcome might be expected for an E1 enzyme such as Uba4 that initiates conjugation but is not required after the event.

The reporter strain PJ69-4A, carrying either Urm1 bait plasmid, was transformed with each of the three AD plasmid libraries (James *et al.,* 1996). Transformants were screened as described in the materials and methods. To be considered as revealing a *bona fide* interaction, a transformant had to activate all three reporters and activation had to be repeated when the AD plasmid was isolated and retransformed into the reporter strain. Only Uba4 was identified in the Gal4BD-Urm1 screen, and two proteins were identified in the Urm1-Gal4BD screen: Ssb1 and Rad30 (Table 3.2).

Concurrent with the transformation-based two-hybrid screen, I collaborated with the Fields lab to perform a two-hybrid using their yeast array. In their genome-wide array each ORF is fused with Gal4AD and carried in distinct haploid yeast strains. Therefore, one can simply mate the array to a yeast strain containing the BD tagged bait and assay reporter activation in the resulting diploids. Both Urm1 bait vectors were sent to the Fields lab, who then performed the two-hybrid screen (Uetz *et al.,* 2000). As with my

two-hybrid screen, the Gal4BD-Urm1 bait only reacted with Gal4AD-Uba4. The Fields lab's screen of Urm1-Gal4BD identified thirteen proteins (Table 3.2).

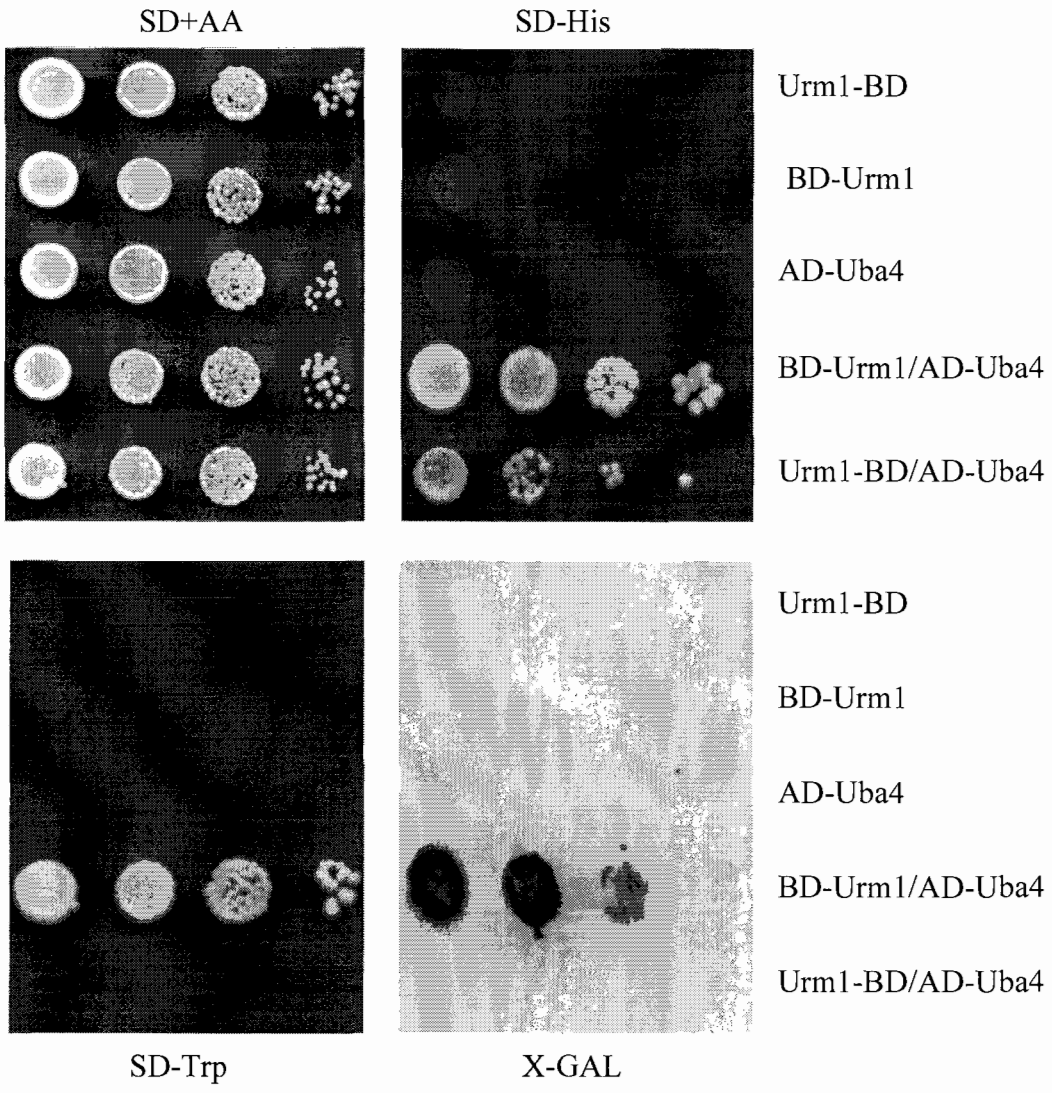

Fig. 3.4. **Testing Gal4BD-Urm1 and Urm1-Gal4BD activation of reporters.** PJ69-4A transformed with CY3925 (Urm1-Gal4BD), CY3950 (Gal4BD-Urm1), and CY3952 (Gal4AD-Urm1). Cells were plated at 0.7 OD_{600} and serially diluted at 1/10 ratios. The *lacZ* reporter was assessed by exposure to X-GAL, as described in the Materials and Methods section.

Table 3.2. **Two-hybrid interactions to Urm1-Gal4BD.** In-lab = CY3925 (Urm1-Gal4BD) in the PJ69-4A reporter strain was transformed with three AD-libraries (James *et al.*, 1996). CY3925 was also sent to the Fields lab for screening using their two-hybrid array (Uetz *et al.*, 2000). Gene descriptions were obtained from the *Saccharomyces* Genome Database, SGD. Color denotes general cellular function: **Transcription, Mitochondria, Actin, Unknown, Transportation, Cell Organization, Degradation.**

Protein	Source	Description
CSE1	Fields	Nuclear envelope protein that mediates the nuclear export of importin alpha.
MER1	Fields	Protein with RNA-binding motifs required for meiosis-specific mRNA splicing.
RAD30	In-lab	DNA polymerase involved in the predominantly error-free bypass replication of DNA lesions.
SLX8	Fields	Subunit of the Slx5-Slx8 SUMO-targeted ubiquitin ligase.
RPL8B	Fields	Ribosomal protein L4 of the large (60S) ribosomal subunit.
AAC3	Fields	Mitochondrial inner membrane ADP/ATP translocator.
MRS3	Fields	Iron transporter that mediates Fe2+ transport across the inner mitochondrial membrane.
SLM6	Fields	Protein with a potential role in actin cytoskeleton organization.
[illegible]	Fields	Protein of unknown function.
[illegible]	Fields	Alpha-1,3-mannosyltransferase, integral membrane glycoprotein of the Golgi.
AVT5	Fields	Putative transporter.
ATG11	Fields	Adapter protein for pexophagy and the cytoplasm-to-vacuole targeting (Cvt) pathway.
OLE1	Fields	Delta(9) fatty acid desaturase.
YCK3	Fields	Vacuolar membrane-localized casein kinase I isoform.
SSB1	In-lab	Cytoplasmic ATPase that is a ribosome-associated molecular chaperone.

The two-hybrid screen provided novel hits from the Urm1-Gal4BD bait only. Because this construct cannot conjugate, it unlikely that any of the hits are Urm1 conjugates. As with the synthetic lethal screen, a good number of hits are related to transcription and transport, but unfortunately none of the two-hybrid hits are known to interact with the synthetic lethal genes. If the two-hybrid interactions are not an artifact

of the Gal4BD fusion, there are two likely reasons for the proteins interacting with Urm1: these proteins may regulate urmylation, or the proteins may recognize Urm1. To determine if any of these proteins regulates urmylation, the non-essential knockouts of each two-hybrid interaction hit was assessed for a change in urmylation determined by a western blot (Figure 3.5). None of the null mutants changed the state of urmylation to any noticeable degree. Determining if the proteins can recognize conjugated Urm1 has the same technical difficulties that were identified in Chapter II, namely the sparse abundance of proteins conjugated with Urm1. It would be unlikely that any pull-down of the two-hybrid hits would detect an Urm1 species, due to the low levels of urmylated species in the cell. In the future, if an Urm1 conjugate was identified that associated with one of the two-hybrid hits, the dependence on urmylation for that interaction could be examined.

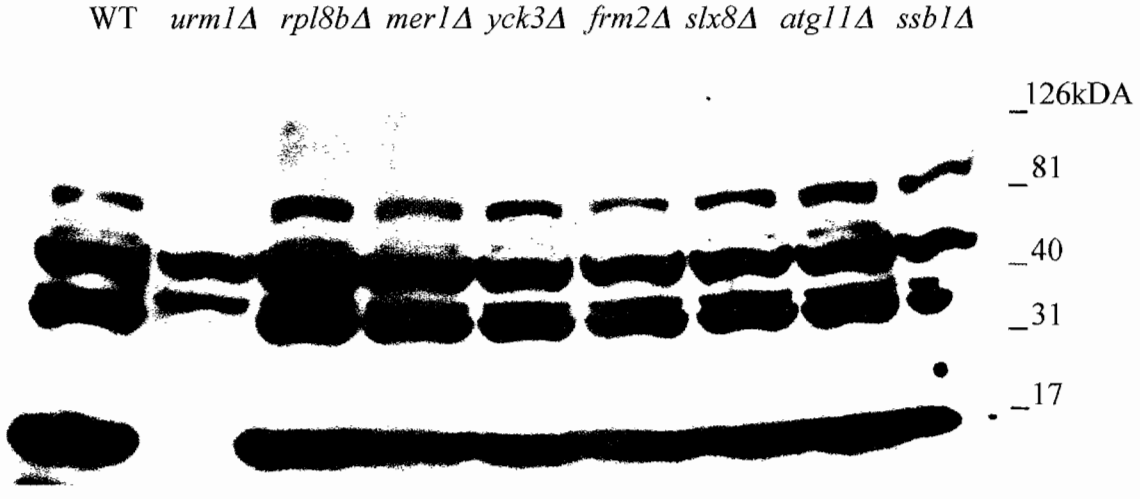

Fig. 3.5. **The state of urmylation in Urm1 two-hybrid hit knockouts.** Whole cell extracts of BY4741 (WT), SY3839 (*urm1Δ*) and a subset of the non-essential two-hybrid hit knockouts were examined by western blot analysis. Probed with Urm1 antibodies.

Two of the two-hybrid hits, Atg11 and Ole1, were also identified in a mass spectrometry screen performed by Kim Landreth. The screen involved a series of immunoprecipitations from yeast cells over-expressing a His-FLAG-Urm1 fusion. The His immunoprecipitation was done following a denaturation step, so only Urm1-

conjugates would have been identified. Unfortunately efforts to detect an urmylated Atg11 or Ole1 by immunoprecipitating tagged fusions of either protein have been unsuccessful.

Screening the Over-Expression Library for Urm1 Regulators

The Andrews lab, in collaboration with the Boone lab, used the same genetic background of the SGA array to create an array of over-expression constructs (Sopko *et al.*, 2006). The over-expression array includes the majority of genes, in which each strain in the array carries a plasmid-borne, galactose-promoter-driven GST tagged gene. If a protein is a negative regulator of urmylation, for example a de-urmylator, its over-expression may mimic an *urm1Δ* mutant. Thus, I screened the over-expression array for sensitivity to diamide stress to identify regulators of urmylation.

I screened the over-expression array a single time for changes in sensitivity to diamide stress. Only strains sensitive to diamide were identified, although it was conceivable the over-expression of particular proteins would increase resistance to the drug. The initial hits were re-examined by dilution series to evaluate their sensitivity to diamide (Figure 3.6). A total of forty proteins caused increased sensitivity to diamide when over-expressed. I chose to focus on ten proteins, which had the best chance of being regulators of urmylation based on their known phenotypes and interactions (Table 3.3). None of the proteins when over-expressed changed the pattern or caused a loss of urmylation, as revealed by western analysis (Figure 3.7). The possibility remains that these proteins regulate the urmylation of conjugates that are not detectable by examination of whole cell extracts.

Table 3.3. **Subset of genes when over-expressed cause sensitivity during diamide stress.** The over-expression array (Sopko *et al.*, 2006) was screened for sensitivity to 1.5mM diamide stress. A subset of genes from the screen are listed here for their potential relevance to Urm1 regulation. Gene descriptions were obtained from the *Saccharomyces* Genome Database, SGD.

GENE	Sensitivity	Description
CRF1	Moderate	Transcriptional corepressor involved in the regulation of ribosomal protein gene transcription via the TOR signaling pathway.
STE20	Mildly	Signal transducing kinase of the PAK.
PHO81	Moderate	Cyclin-dependent kinase (CDK) inhibitor.
SNX41	Mildly	Sorting nexin, involved in the retrieval of late-Golgi SNAREs from the post-Golgi endosome to the trans-Golgi.
UBX4	moderate	UBX (ubiquitin regulatory X) domain-containing protein that interacts with Cdc48.
MPM1	Mildly	Mitochondrial membrane protein of unknown function.
RRI1	Moderate	Catalytic subunit of the COP9 signalosome acts as an isopeptidase in cleaving the ubiquitin-like protein Nedd8.

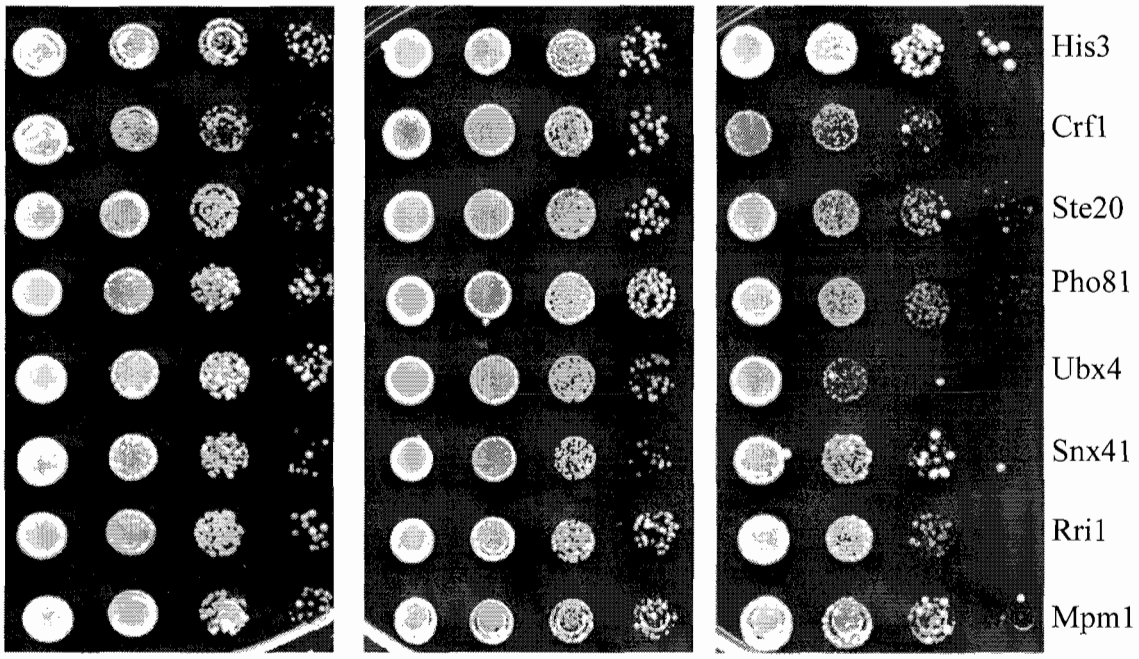

Fig. 3.6. **Secondary screen of the over-expression array to diamide stress.** Serial dilutions of over-expression strains initially identified as sensitive to 1.5mM diamide on the array. The His3 vector from the over-expression array served as a control, cells were plated at 0.7 OD_{600} and serially diluted at 1/10 ratios.

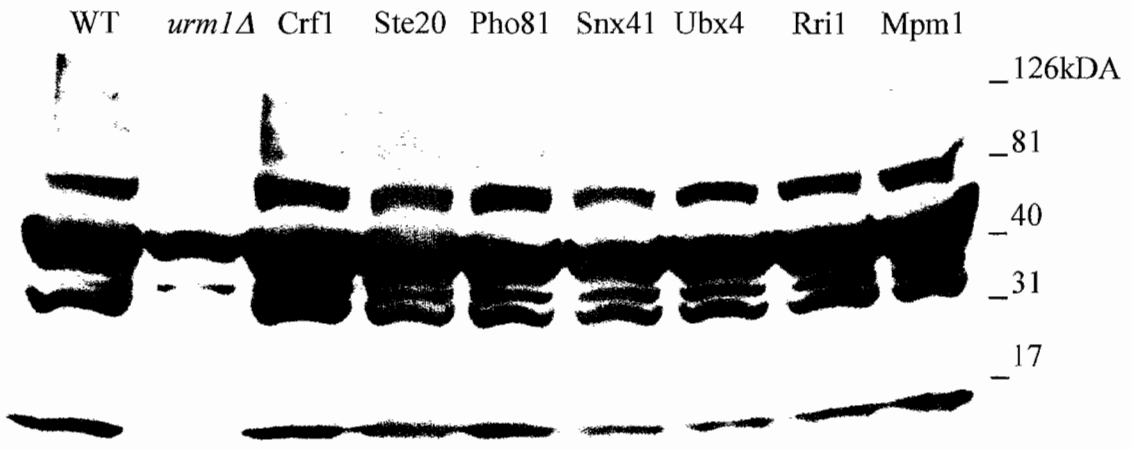

Fig. 3.7. **The state of urmylation during over-expression of proteins.** Whole cell extract from strains BY4741 (WT), SY3839 (*urm1Δ*) and strains isolated from the over-expression array Gal-induced for 4hours. Extracts were examined by western blot probed with the Urm1 antibody.

Identifying Urm1 Conjugates

In addition to Atg11 and Ole1, I examined a subset of proteins identified from the mass spectrometry of the His-FLAG-Urm1 immunoprecipitates, preformed by Kim Landreth (Table 3.4). The subset of proteins was chosen based on two criteria: the probability that the protein identified in mass spectrometry was *bona fide*, and the likelihood of conjugation to Urm1 based on each protein's phenotypes and interactions. To examine each protein for urmylation, GST tagged plasmids from the over-expression array (Sopko *et al.*, 2006) were isolated and then transformed into BY4741, which was also over-expresses Urm1 via the tetracycline promoter vector CY3937. A GST pull down isolated each GST-protein and the existence of a urmylated species was assessed by western analysis probed with the Urm1 antibody. Only one protein was identified as a conjugate, the Elongator complex component, Elp2, which will be discussed in Chapter IV.

Table 3.4. **Urm1 immunoprecipitation mass spectrometry screen.** A subset of predicted peptides from mass spectrometry analysis of 6XHIS-FLAG-Urm1 immunoprecipitation. Gene descriptions were obtained from the *Saccharomyces* Genome Database, SGD.

Protein	Description
Ole1	Delta(9) fatty acid desaturase.
Atg11	Adapter protein for pexophagy and the cytoplasm-to-vacuole targeting (Cvt) pathway.
Cog3	Essential component of the conserved oligomeric Golgi complex.
Cog8	Essential component of the conserved oligomeric Golgi complex.
Ksp1	Ser/thr protein kinase; nuclear translocation required for haploid filamentous growth.
Pex3	Peroxisomal membrane protein.
Rpn9	Non-ATPase regulatory subunit of the 26S proteasome.
Ifh1	Essential protein; potential Cdc28p substrate.
Sit4	Serine-threonine phosphatase.
Ssa2	ATP binding protein involved in protein folding; member of heat shock protein 70 (HSP70) family.
Elp2	Subunit of Elongator complex.

Conclusion

I have completed three screens to further investigate the role of Urm1 and to identify targets or regulators of urmylation: a synthetic lethal screen, a two-hybrid screen, and an over-expression screen for sensitivity to diamide stress. The synthetic lethal screen potentially implicates Urm1 in transcription and translational events. Of particular interest was the identification of five of the six components of the Elongator complex. The ramifications of this identification will be discussed further in Chapter IV. One other synthetic lethal interaction, *PTC1,* is potentially informative. Ptc1's regulation of the MAPK Hog1 has intriguing possibilities for the role of Urm1 as a regulator of MAPK pathways. Analysis of the *PTC1* synthetic lethal interaction will be further explored in Chapter IV. The two-hybrid screen provided several interesting hits, but none of them could be directly linked back to Urm1, due in large part to the technical difficulties of the

project. The list of proteins may still prove useful as additional Urm1 conjugates are identified. The over-expression screen failed to identify any regulators of urmylation. As with the two-hybrid screen, the list of identified genes may prove useful if additional targets of urmylation are discovered; the proteins identified may only regulate the urmylation of one target, whose low abundance precludes detected by a western blot directly. Overall, the efforts to screen *S. cerevisiae* for information on Urm1 brought two important leads for my project: the Elongator complex and *PTC1*.

CHAPTER IV
THE IMPLICATIONS OF URM1 AS A SULFUR CARRIER

Introduction

The understanding of Urm1's function took an unexpected turn with the discovery that it serves as a sulfur donor for the thiolation of a wobble position base in some tRNAs, U_{34}. The U_{34} wobble position is almost always modified in the cell and is part of the codon specifying three amino acids: lysine, glutamine and glutamic acid (Bjork *et al.*, 1999). Of the potential modifications of the U_{34} wobble position, I will discuss methylation (5-methoxycarbonylmethyluridine mcm^5U_{34}), thiolation (5-methoxycarbonyl-2-thiouridien $mcm^5s^2U_{34}$) and amidation (5-carbamoylmethyluridine ncm^5U_{34}) (Figure 4.1) (Bjork *et al.*, 1999). An unmodified U_{34} has the potential to recognize any nucleotide base (Agris *et al.*, 1991). The presence of modifications on the U_{34} position restricts wobble recognition to A- and G- ending codons and loss of these modifications will result in a general reduction in the efficiency of translation of such codons (Lim *et al.*, 1994). In addition to directly affecting the mechanics of translation, these modifications are also thought to alter the half-life of tRNAs and fine-tune their interactions with mRNAs and ribosomes (Agris *et al.*, 2008; Wang *et al.*, 2007; Bjork *et al.*, 2007; Johansson *et al.*, 2008).

Three lines of evidence point to Urm1 as being required for the $mcm^5s^2U_{34}$ tRNA modifications. First, to identify genes responsible for the $mcm^5s^2U_{34}$ tRNA modification, the Huang group screened the yeast deletion collection for resistance to the γ-subunit of zymocin from *K. lactis* and identified *URM1* (Huang *et al.*, 2008). The γ-subunit is an endonuclease that requires the $mcm^5s^2U_{34}$ modification in order to function, and loss of the tRNA modification protects yeast strains from γ-subunit's lethal affects (Lu *et al.*, 2005). Second, the Nakai group identified Ncs6's (Need Cla4 to Survive) involvement in tRNA modification based on its homology to other tRNA interacting proteins.

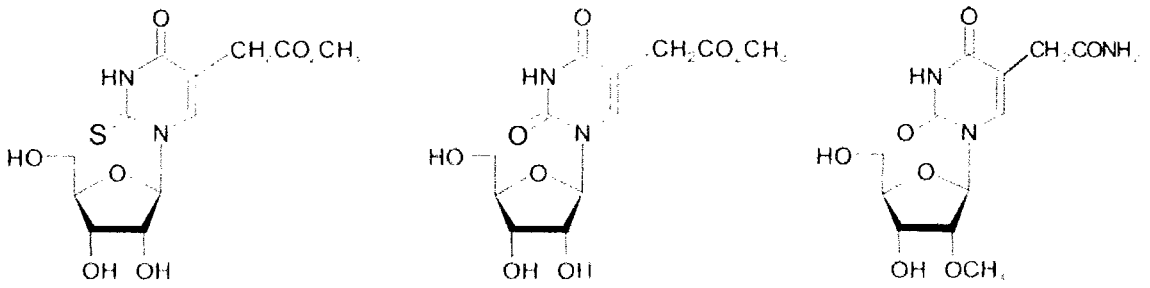

Fig. 4.1. **tRNA modifications dependent on the Elongator complex.** The three identified tRNA modifications dependent on the Elongator complex: 5-methoxycarbonylmethyluridine (mcm^5U_{34}), 5-methoxycarbonyl-2-thiouridien ($mcm^5s^2U_{34}$) and 5-carbamoylmethyluridine (ncm^5U_{34}). Only $mcm^5s^2U_{34}$ is dependent on the urmylation system. Figure from Huang et al 2004.

Reasoning that other *cla4Δ* synthetic lethal interactions could be related to tRNA modifications, the group identified a dependence of $mcm^5s^2U_{34}$ modification on Urm1 and Uba4 (Nakai *et al.*, 2008). Third, independent of my synthetic lethal screen, the Leidel group found that simultaneous loss of Urm1 and the Elongator complex was lethal, prompting them to examine Urm1's role in tRNA modification (Leidel *et al.*, 2009). All three groups identified the dependence of the $mcm^5s^2U_{34}$ modification of tRNA on Urm1.

An *urm1Δ* mutant only disrupts the $mcm^5s^2U_{34}$ modification; mcm^5U_{34} and ncm^5U_{34} levels remain unchanged (Huang *et al.*, 2008). The role of Urm1 as a sulfur carrier is supported by studies of Urm1's structure: Urm1 has a greater similarity to the *E. coli* sulfur transfer proteins MoaD and ThiS than to ubiquitin (Singh *et al.*, 2005; Xu *et al.*, 2006). Urm1's E1 activating enzyme, Uba4, likewise shares greater sequence similarity to the *E. coli* protein MoeB than to E1 activating enzymes involved in ubiquitin conjugation (Schmitz *et al.*, 2008). To determine if Uba4 behaved as an E1 or as a MoeB-like sulfur transfer protein, Schmitz and collaborators examined Uba4's interaction with Urm1 *in vitro*. Disrupting Uba4's rhodanese domain, a domain found in MoeB but not eukaryotic E1s, eliminated the detection of the Uba4/Urm1 complex. In contrast, a

mutation of the predicted E1 active site had no effect (Schmitz *et al.*, 2008). The Schmitz group was unable to detect a thioester bond between Uba4 and Urm1, although they were able to detect this bond between ubiquitin and its E1 (Schmitz *et al.*, 2008). Either by mass spectrometry (Schmitz *et al.*, 2008) or by following the transfer of S^{35} to Urm1 (Leidel *et al.*, 2009), both the Schmitz and Leidel groups were able to detect a Uba4 dependent transfer of a thiocarboxylate to Urm1's C-terminus *in vitro*, showing that Urm1 can act as a sulfur carrier.

The Elongator complex is required for the ncm^5U_{34}, mcm^5U_{34}, and $mcm^5s^2U_{34}$ tRNA modifications. The latter modification can only be made on tRNAs that carry the mcm^5U_{34} modification (Figure 4.1) (Huang *et al.*, 2005). The temperature sensitivity of Elongator null mutants can be suppressed by the over-expression of tRNAs that undergo these modifications (lysine, glutamine and glutamic acid), presumably because over-expression overcomes the translational defects (Froholoff *et al.*, 2001; Esberg *et al.*, 2006). Interestingly, over-expression of these tRNAs also suppressed other defects of Elongator mutants. In particular, transport of Sec2 was restored as was transcription of Elongator dependent genes (Esberg *et al.*, 2006). These findings suggest that the main function of the Elongator complex is tRNA modification and the other functions associated with the complex are dependent on presence of these modified tRNAs.

It has become clear that it is Urm1's ability to transfer sulfur that is critical for the $mcm^5s^2U_{34}$ tRNA modification. The Liedel group examined the suppression of *urm1Δ* phenotypes by the over-expression lysine and glutamic acid isoaccepter tRNAs (Liedel *et al.*, 2009). Sensitivity to diamide and rapamycin was suppressed by over-expression of the tRNAs in both *urm1Δ* and *uba4Δ* backgrounds (Liedel *et al.*, 2009). Given that two known *urm1Δ* phenotypes can be suppressed by the over-expression of tRNAs, a natural question is whether conjugation of target proteins by Urm1 is important. Indeed, many Elongator mutants have been identified in screens for phenotypes such as rapamycin sensitivity, diamide sensitivity and inability to undergo filamentous growth, phenotypes also exhibited by *urm1Δ* mutants (Xie *et al.*, 2005; Thorpe *et al.*, 2004; Jin *et al.*, 2008).

In conclusion, the accumulated literature supports a model in which Urm1 serves as a sulfur transfer protein. Urm1 and its E1, Uba4, align more closely with the *E. coli* sulfur transfer proteins MoeD and MoeB than with congruent ubiquitin proteins. The transfer of sulfur to Urm1 by Uba4 could be detected *in vitro*, whereas the conjugation dependent thioester bond could not. Unlike the Elongator complex, Urm1 is only required for the thiolation of mcm^5U_{34}, again suggesting Urm1's most critical role is the ability to act as a sulfur donor.

The above arguments however do not preclude a role for Urm1 conjugation. I therefore decided to test the known phenotypes of the *urm1Δ* mutant, as well as any new phenotypes I could identify, to determine if any could not be suppressed by tRNA over-expression and therefore might be independent of the tRNA modification defect. To date all Urm1 dependent processes I have examined are suppressed by tRNA over production, lending support to the idea that the main role of Urm1 is to act as a sulfur donor in the modification of tRNA.

The Role of Urm1 in Hog1 Activation

Ptc1, as described in Chapter III, is a Ser/Thr phosphatase whose absence leads to a synthetic sick phenotype if Urm1 is also absent. One target of Ptc1 is the MAPK Hog1, which is part of a pathway that responds to osmostress (Warmka *et al.*, 2001). In response to extracellular high osmolarity, this pathway transduces the extracellular signal from a membrane protein to a cascade of protein kinases: a MAPKKK, a MAPKK, and finally a MAPK, which activates proteins that ameliorate the stress (Gustin *et al.*, 1998). Two residues on Hog1 must be phosphorylated, tyrosine176 (pY) and threonine 174 (pT), to activate Hog1 (Brewster *et al.*, 1993). Ptc1 is one of a set of Ser/Thr phosphatases that targets the Hog1 pT site; the pY site is targeted by a separate set of protein tyrosine phosphatases (Warmaka *et al.*, 2001; Jacoby *et al.*, 1997). Loss of Ptc1 in combination with the other phosphatases that negatively control Hog1 constitutively activates Hog1, leading to sick or lethal strains (Warmka *et al.*, 2001). Is the sick phenotype of the *ptc1Δurm1Δ* mutant related to the activation of Hog1?

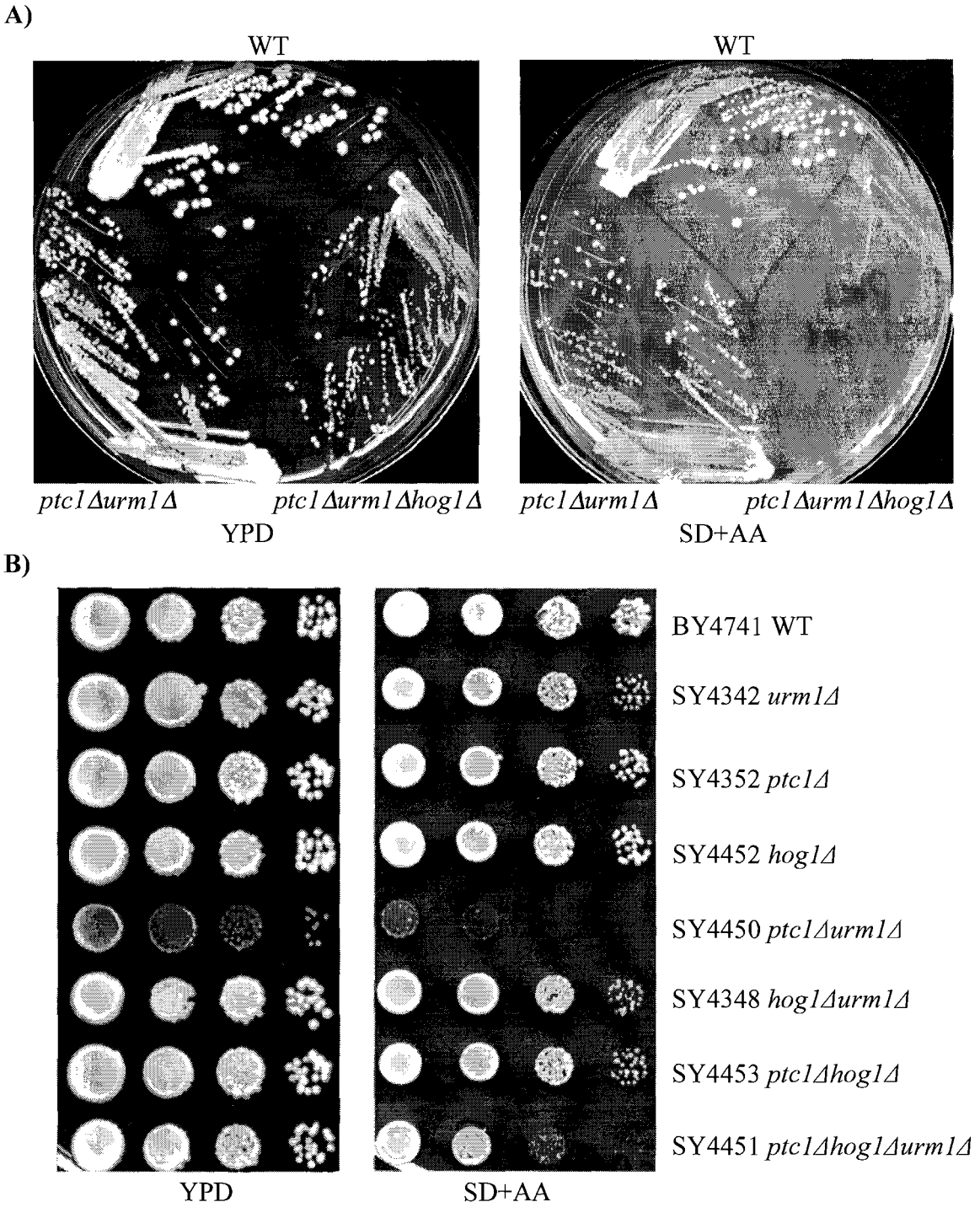

Fig. 4.2. **Suppression of the *urm1Δptc1Δ* fitness defect by the loss of Hog1.** The loss of Hog1 suppressed the *urm1Δptc1Δ* synthetic sick phenotype. Plates were grown for 3 days at 30°C. **A)** Streak purification for single yeast colonies **B)** Cells were plated at 0.7 OD_{600} and serially diluted at 1/10 ratios.

If the activation of Hog1 is responsible for the fitness defect of *ptc1Δurm1Δ* mutants, the triple mutant *ptc1Δurm1Δhog1Δ* should exhibit improved fitness (Figure 4.2 A,B). Indeed, I found that loss of Hog1 led to a partial restoration of growth in the *ptc1Δurm1Δ* background. Although wild-type growth was not restored, the partial restoration suggests there may be other pathways affected by the *PTC1 URM1* genetic interaction. To examine whether the regulation of Hog1 changed in an *urm1Δ* mutant as the above result suggested, I followed the phosphorylation of the pY site on Hog1, using an antibody specific to pY 176, (Figure 4.3). There was no change in the phosphorylation of the pY site in the absence of salt stress in an *urm1Δ* mutant. However, as the level of salt stress increased, Hog1 was phosphorylated at lower concentration in *urm1Δ* cell than in wild-type cells, 0.2M NaCl stress (Figure 4.3). Sensitized phosphorylation of Hog1 in an *urm1Δ* background may suggest that Urm1 serves to fine-tune the signal of osmostress, possibly by involvement in the regulation of the phosphatases themselves.

It was important to ask whether the phosphorylation change of Hog1 in an *urm1Δ* mutant led to a increase in signaling in the Hog1 pathway, as would be expected. I followed the transcriptional activation of the *lacZ* driven by the *STL1* promoter (developed by Claire Romelfanger, Sprague laboratory), a gene whose transcription is tightly controlled by the Hog1 pathway (Posas *et al.*, 2000) (Figure 4.4 A,B). Consistent with the expectation, the loss of Urm1 stimulated transcription of the reporter by about two-fold in the presence of 1M salt and two-fold above basal levels in 0M salt, suggesting that the pathway is more easily activated in the absence of a potential regulator. Loss of the phosphatase Ptc1 increases *STL1* activation in the absence of salt stress and in the presence of 1M NaCl, in both cases by a factor of five compared to the wild-type (Figure 4.4 A,B). The *ptc1Δurm1Δ* double mutant showed greater activation of the reporter than either single mutant in 0M salt, around seven fold more than seen for wild-type (Figure 4.4 A,B). In the *ptc1Δurm1Δ* mutant, 1M NaCl stimulated *STL1* activity less than in the *ptc1Δ* strain. This finding may be a consequence of the reduced fitness of the double mutant compared to the *ptc1Δ* single mutant. That loss of both genes produced an additive effect implies that Urm1 and Ptc1 have separate roles in regulating

the Hog1 pathway. Urm1's role in the does not appear to be as substantial as that of the Ptc1 phosphatase.

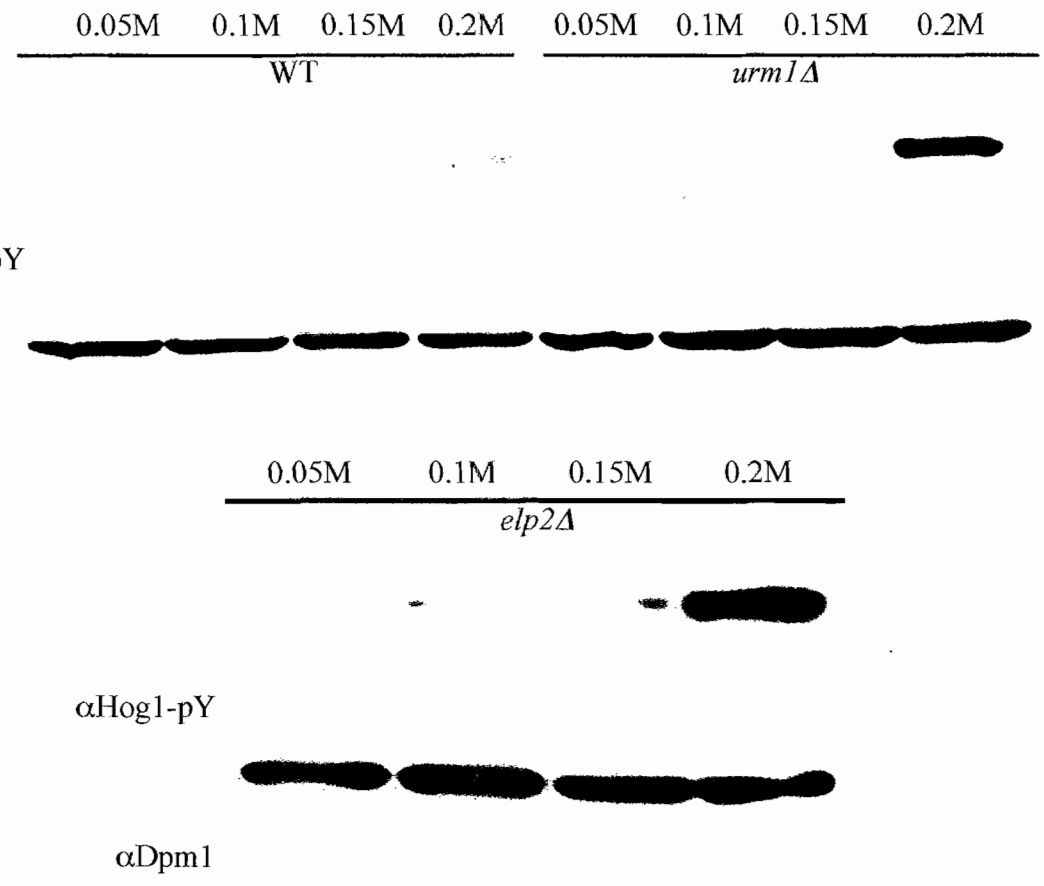

Fig. 4.3. **The state of Hog1 phosphorylation in *urm1Δ* and *elp2Δ* mutants.** BY4741(WT), SY3839 (*urm1Δ*), SY4478 (*elp2Δ*) were grown to mid-log in YPD media then exposed to varying levels of NaCl stress for 10minutes. Protein was isolated via TCA extraction, described in Materials and Methods section, and examined by western analysis. Phosphorylation of Hog1 was detected using the antibody specific to Hog1's pY site. The Dpn1 antibody was used to determine relative protein concentration.

A)

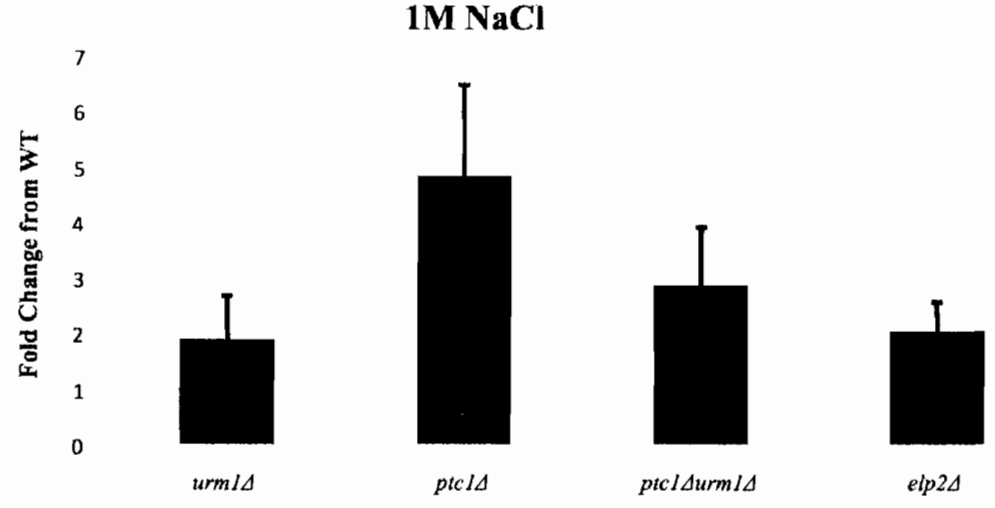

B)

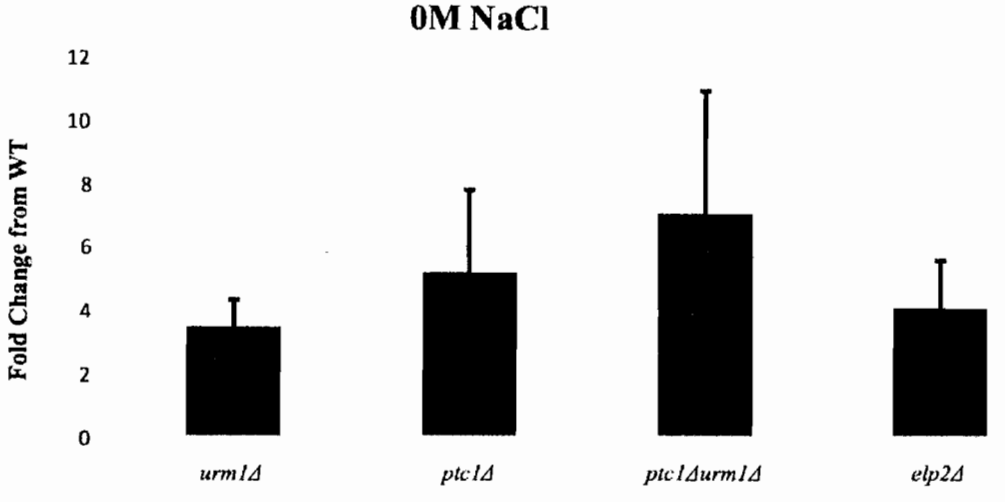

Fig. 4.4 **The change in β-galactosidase activity of the Hog1 dependent *STL1 lacZ* reporter in the absence or presence of 1M NaCl .** BY4741 (WT), SY3839 (*urm1Δ*), SY4342 (*ptc1Δ*), SY4450 (*ptc1Δurm1Δ*), SY4478 (*elp2Δ*), expressing CY4016 (P_{STL1} *lacZ*). The fold change represents the change in miller units of each strain compared to the wild-type. **A)** Strains were exposed to 1M NaCl. **B)** Strains were not exposed to salt.

To determine if Urm1's role in the Hog1 pathway could be ascribed to its role in tRNA modification, I asked whether loss of Elp2, also required for tRNA modifications, affected Hog1 pathway signaling. Loss of the Elongator component Elp2 led to an increased level of pY Hog1 phosphorylation at 0.2M salt and activated the *STL1* reporter to a similar degree as seen in the *urm1Δ* mutant (Figure 4.3). Given that this finding implicates the Elongator complex and its main function tRNA modification in the regulation of the Hog1 pathway, I examined whether the over-expression of tRNAs affected the fitness of the *ptc1Δurm1Δ* strain (Figure 4.5). Over-expression of the tRNAs partially suppressed the fitness defect of the *ptc1Δurm1Δ* strain. I conclude therefore that the affect of the *urm1Δ* strain on the regulation of the Hog1 pathway is very likely to be a consequence of the loss of tRNA modification rather than a direct relationship of Urm1 with the pathway. Loss of the tRNA modification could affect the translation of regulatory proteins and disrupt the balance of signaling.

Screening for *urm1Δ* Phenotypes Independent of Loss of tRNA Modifications

Loss of tRNA modifications could explain the diverse phenotypes associated with *urm1Δ* mutants as changes in translation can have global affects on the cell. I examined whether over-expression of tRNAs could suppress the known phenotypes of an *urm1Δ* mutant: sensitivity to high temperature, sensitivity to oleate, sensitivity to rapamycin, sensitivity to diamide, and loss of filamentous growth (Furukawa *et al.*, 2000; Goehring *et al.*, 2003; Lockshon *et al.*, 2007). I used two criteria to ask if phenotypes are dependent on tRNA modification: first, do Elongator null mutants share the *urm1Δ* phenotypes, and second, are the mutants' phenotypes suppressed by over-expression of tRNAs?

I also screened for new phenotypes of an *urm1Δ* mutant by testing conditions suggested by genes identified in the screens carried out in Chapter III. I then assessed if tRNAs could suppress these new phenotypes. I found that *urm1Δ* mutants are sensitive to latrunculinA (LatA), phelomycin, and tergitol. *urm1Δ* mutants also show a general fitness defect on poor carbon sources. All of the *urm1Δ* mutant phenotypes I examined were suppressed by tRNA over-expression.

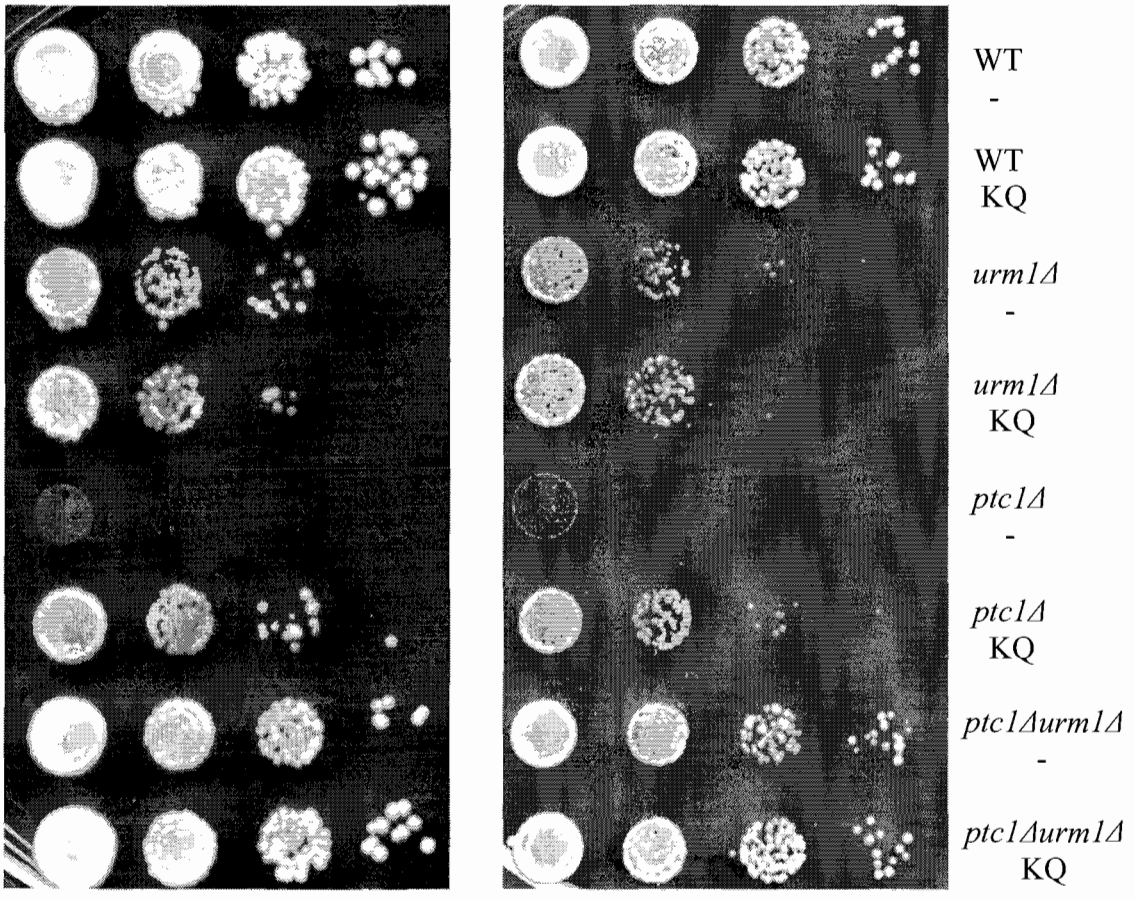

Fig. 4.5. **Over-expression of tRNAs K & Q partially suppresses a *ptc1Δurm1Δ* mutant.** BY4741 (WT), SY3839 (*urm1Δ*), SY4342 (*ptc1Δ*), and SY4450 (*ptc1Δurm1Δ*) were transformed with either the CY4035 (-) the empty plasmid or CY4034 (KQ) tRNAs. Cells were plated at 0.7 OD_{600} and serially diluted at 1/10 ratios.

One of the first *urm1Δ* mutant phenotypes discovered was temperature-sensitive growth (Furukawa *et al.*, 2000), and as expected, the *urm1Δ* and *uba4Δ* stains' sensitivity were suppressed by expression of tRNAs (Figure 4.6). *urm1Δ* and *uba4Δ* strains were not as sensitive to heat stress as the Elongator mutants (Figure 4.6). In confirmation of work from the Liedel group, I found that *urm1Δ* and *uba4Δ* sensitivity to diamide and rapamycin was also suppressed by tRNA over-expression (Figure 4.6) (Liedel *et al.*, 2009). Analysis of null mutant for each member of the Elongator complex (except Elp5, as its null is lethal in the BY4741) confirmed that loss of any Elongator gene leads to similar levels of sensitivity to either drug. The Elongator null mutants drug sensitivity could also be suppressed by over-expression of tRNAs (Figure 4.6). Loss of any of the Elongator genes disrupted filamentous growth, as assessed by plate invasion (Figure 4.7 A). Expression of the tRNAs restored the plate invasion of an *urm1Δ* mutant (Figure 4.7 B). In conclusion, all of the published *urm1Δ* phenotypes can be explained by the disruption of tRNA modification.

A previous screen of the yeast deletion collection for mutants sensitive to oleate identified *URM1* (Lockshon *et al.*, 2007). I examined in detail the sensitivity of *urm1Δ* and *uba4Δ* mutants to oleate and discovered that oleate was not responsible for the observed sensitivity but the detergent, tergitol, placed in the media to allow dispersion of oleate. I compared urmylation null strains grown on YP media (yeast extract and peptone), YP + tergitol media (YPT), and YP + tergitol and oleate media (YPTO) (Figure 4.8 A). The *urm1Δ* or *uba4Δ* mutants had a fitness defect on media lacking carbon, YP. This fitness defect increased in the presence of tergitol but did not change in the presence of oleate. Interestingly, the Elongator nulls did not exactly share the same pattern of phenotypes with the urmylation mutants. Whereas the fitness defect on YP media was similar to urmylation mutants, the same addition of tergitol did not exacerbate the Elongator mutants' phenotypes (Figure 4.8 A). Although *urm1Δ and elpΔ* mutants had different phenotypes on tergitol, tRNA over-expression suppressed the fitness defect of growth on YPT of a *urm1Δ* strain (Figure 4.8 B).

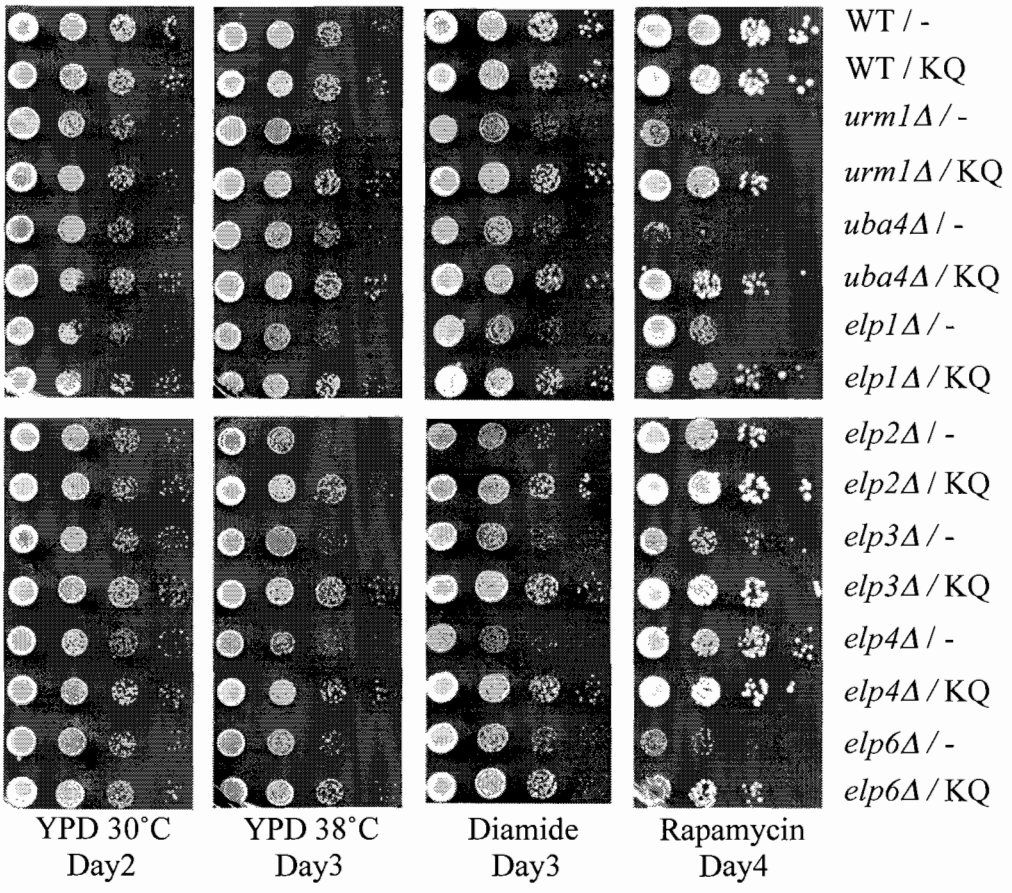

Fig. 4.6. **Over-expression of tRNAs K & Q suppresses temperature, diamide, and rapamycin sensitivity.** BY4741 (WT) was the background strain. Strains were transformed with either the CY4035 (-) the empty plasmid or CY4034 (KQ) tRNAs. Strains were plated at 0.7 OD_{600} and serially diluted at 1/10 ratios. 1.0mM diamide was added to YPD plates. 1nM rapamycin was added to YPD plates.

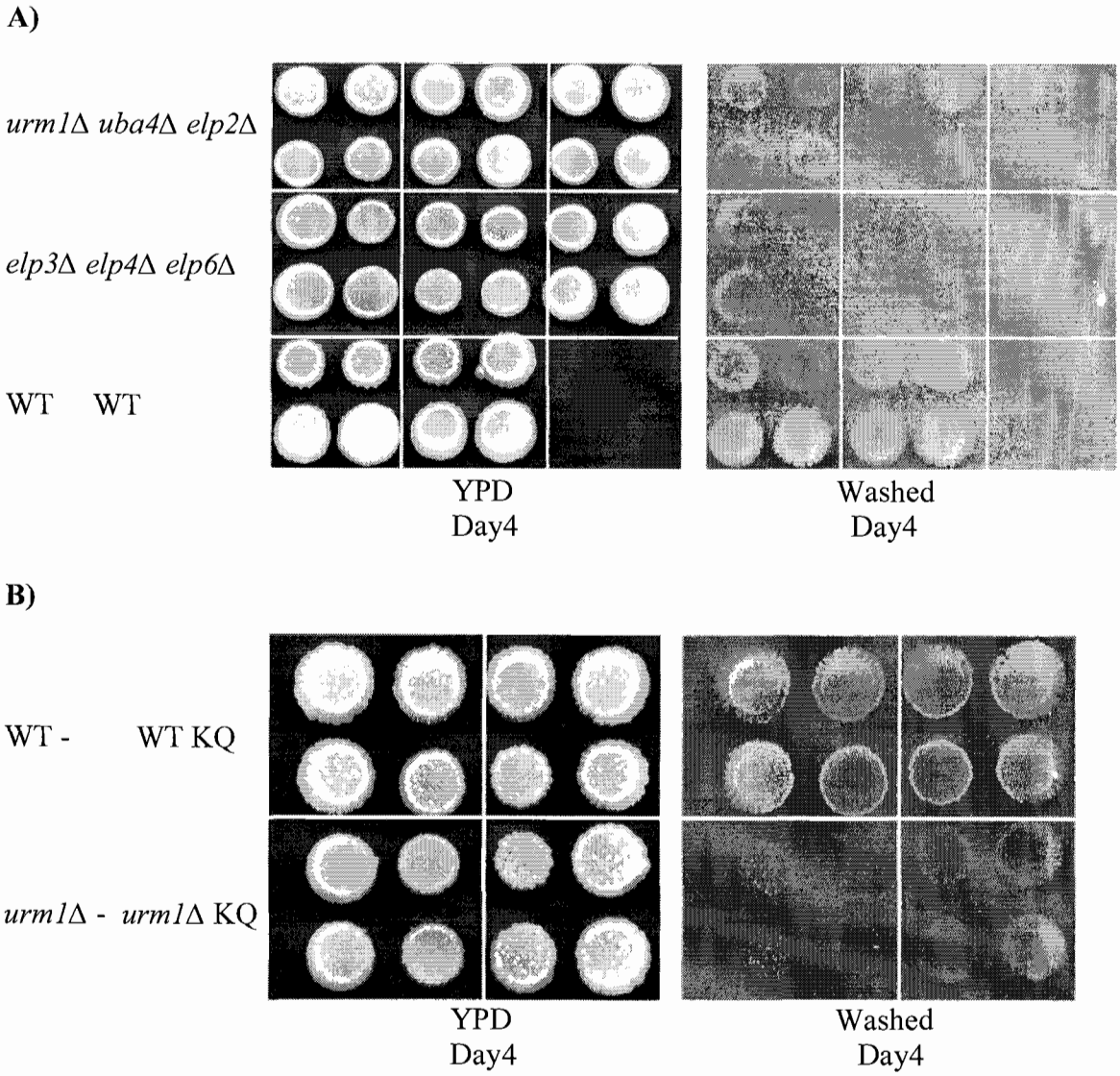

Fig. 4.7. **The dependency of filamentous growth on the Elongator complex and tRNA modification.** Strains were grown to mid-log and plated at 0.7 OD_{600}. Strains that grow filamentously will invade the agar and leave a scar after plate washing. **A)** Loss of urmylation or Elongator components disrupts filamentous growth. Strains are from the Sigma background **B)** Over-expression of CY4934 (KQ) tRNAs restore filamentous growth in an *urm1*Δ mutant in the HYL333 background.

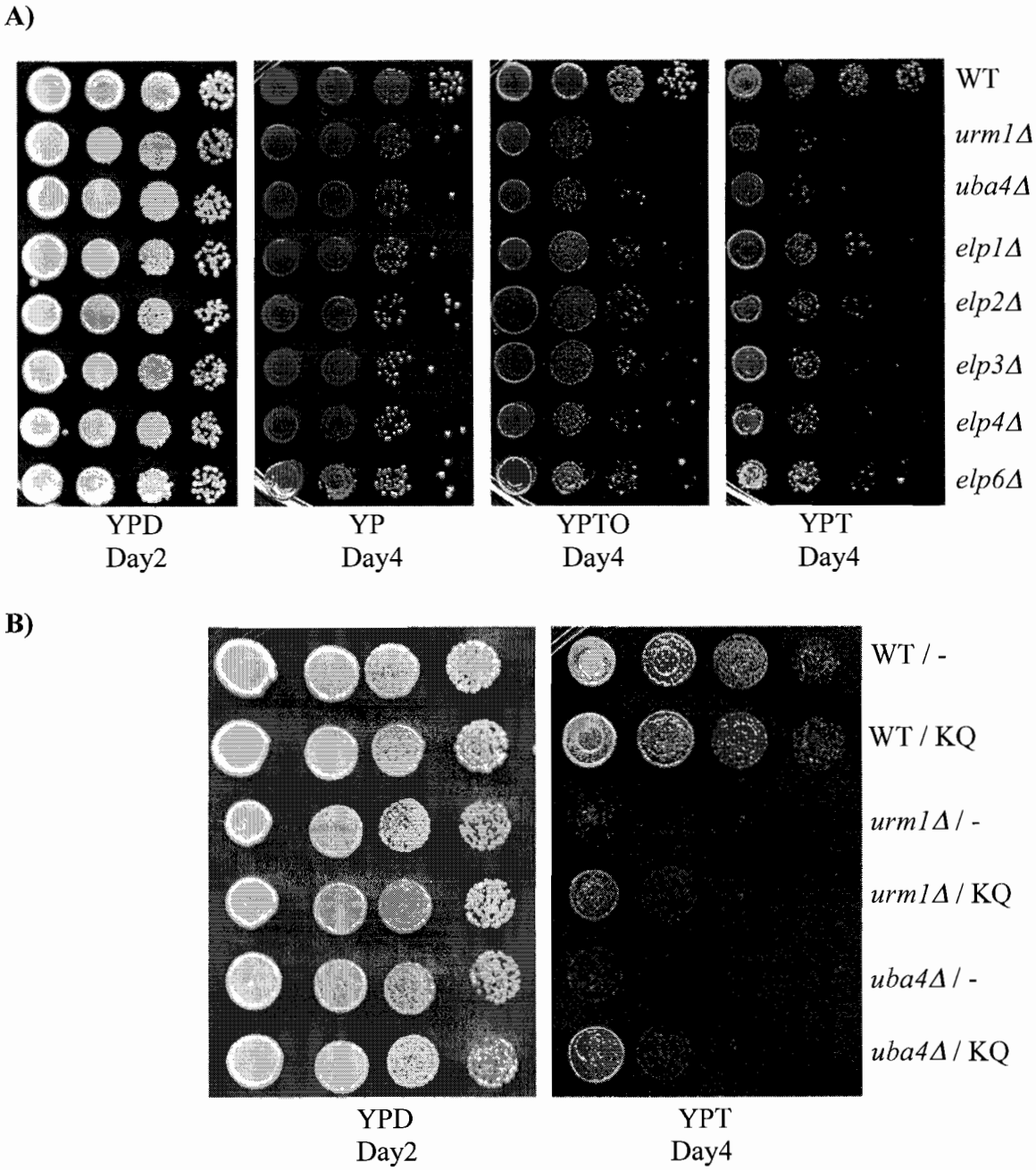

Fig. 4.8. **Sensitivity of urmylation mutants to oleate media is due to tergitol, but can be partially suppressed by over-expression of tRNAs.** BY4741 (WT) was the background strain. Strains were plated at 0.7 OD_{600} and serially diluted at 1/5 ratios. **A)** Comparing urmylation to Elongator mutants on YP, tergitol, and oleate media. **B)** Strains were transformed with either the CY4035 (-) the empty plasmid or CY4034 (KQ) tRNAs.

I also examined the ability of urmylation and Elongator null mutants to respire on poor carbon sources compared the wild-type background strain, BY4741. I examined a set of carbon options: galactose, raffinose, maltose, lactic acid, glycerol, EtOH and the addition of no carbon. Each null mutant grew less well on these poor carbon sources than did wild-type (Figure 4.9, 4.10). The carbon growth defects were suppressed by over-expression of the tRNAs in urmylation and Elongator mutants (Figure 4.9, 4.10). One interesting observation, however, is that the *urm1Δ* and *uba4Δ* strains were more defective at growth on maltose than the Elongator complex mutants, but this phenotype still suppressed when tRNAs were over-expressed (Figure 4.11).

In Chapter III, I identified a number of genes that show interaction with *URM1*. I asked whether *urm1Δ* mutants might exhibit phenotypes suggested by these interactions. Indeed, loss of Urm1 led to sensitivity to the DNA-damaging drug phelomycin and the actin de-polymerizing drug LatA. Both urmylation and Elongator mutants were sensitive to phelomycin, however the *urm1Δ* mutant was significantly more sensitive than the Elongator mutants (Figure 4.11). The phelomycin phenotype was suppressed by over-expression of tRNAs (Figure 4.11). The sensitivity to LatA was determined by a halo assay in which the diameter of growth inhibition caused by the drug was measured (Figure 4.12 A,B). The *urm1Δ* mutant was 7% more sensitive to LatA than were wild-type cells; *elp2Δ* was 12% more sensitive. The LatA sensitivity of both mutants were suppressed by the expression of the tRNAs, the *urm1Δ* mutant's diameter was restored to that of wild type and the *elp2Δ* mutant was restored to within 5% that of the wild-type (Figure 4.12 A,B).

The Urm1 Conjugation of Elp2

One interesting protein identified in Kim Landreth's Urm1 mass spectrometry screen was Elp2. A GST immunoprecipitation of the GST-Elp2 construct pulled down an urmylated species of the correct size, as detected by the Urm1 antibody (Figure 4.13). To assure the urmylated band indeed corresponded to Elp2, the construct was also tagged with GFP and a new urmylated band was observed at the expected size (Figure 4.13).

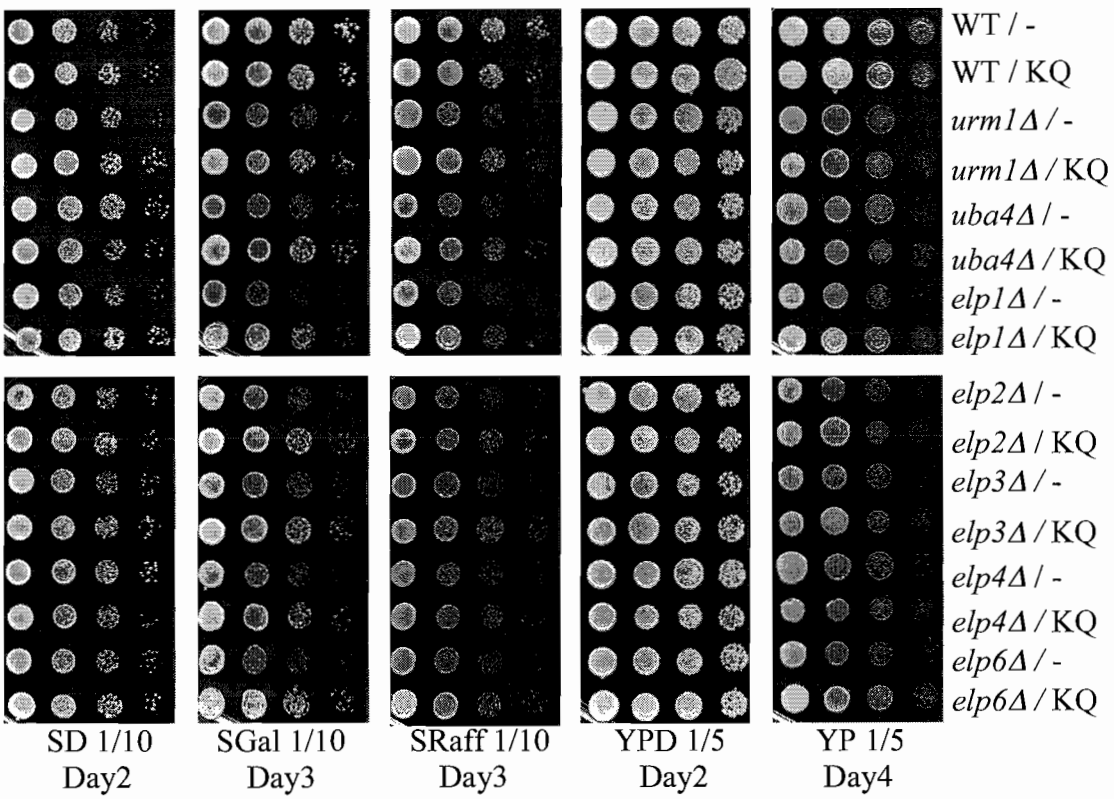

Fig. 4.9. **Fitness defects of urmylation and Elongator mutants grown on galactose, raffinose, and YP media are suppressed by the over-expression of tRNAs.** BY4741 (WT) was the background strain. Strains were transformed with either the CY4035 (-) the empty plasmid or CY4034 (KQ) tRNAs. Strains were plated at 0.7 OD_{600} and serially diluted at ratios listed.

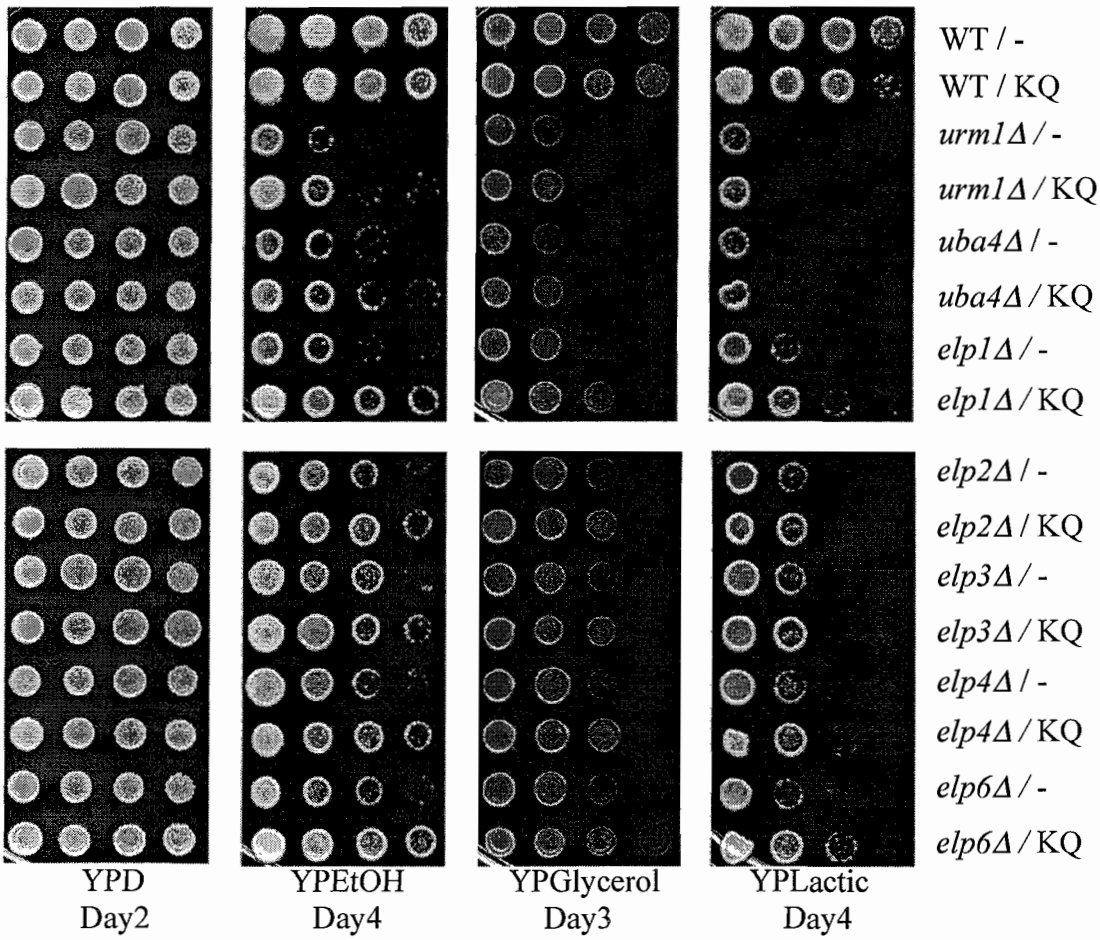

Fig. 4.10. **Fitness defects of urmylation and Elongator mutants grown on EtOH, glycerol, and lactic acid media are suppressed by the over-expression of tRNAs.** BY4741 (WT) was the background strain. Strains were transformed with either the CY4035 (-) the empty plasmid or CY4034 (KQ) tRNAs. Serial dilutions were diluted in the ratios listed. EtOH, Glycerol and Lactic Acid. Strains were plated at 0.7 OD_{600} and serially diluted at 1/2 ratios.

A)

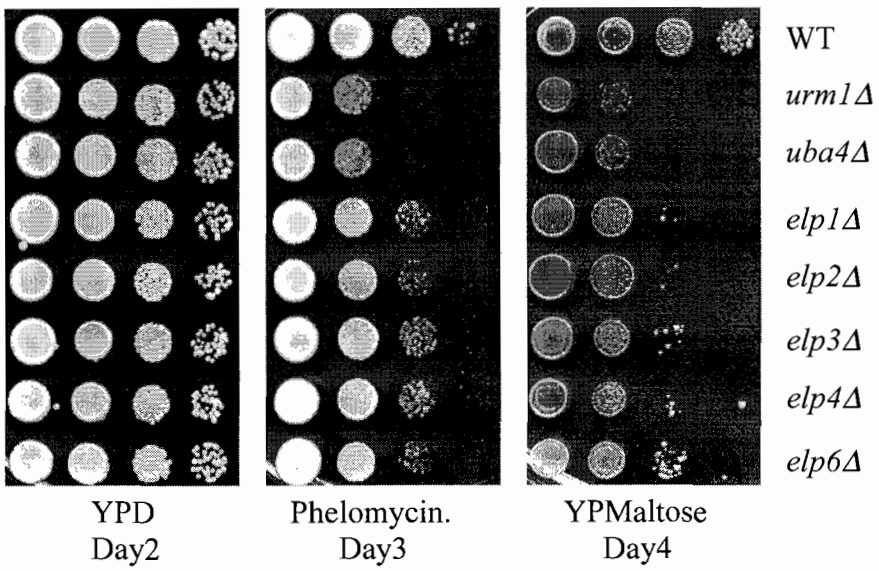

B)

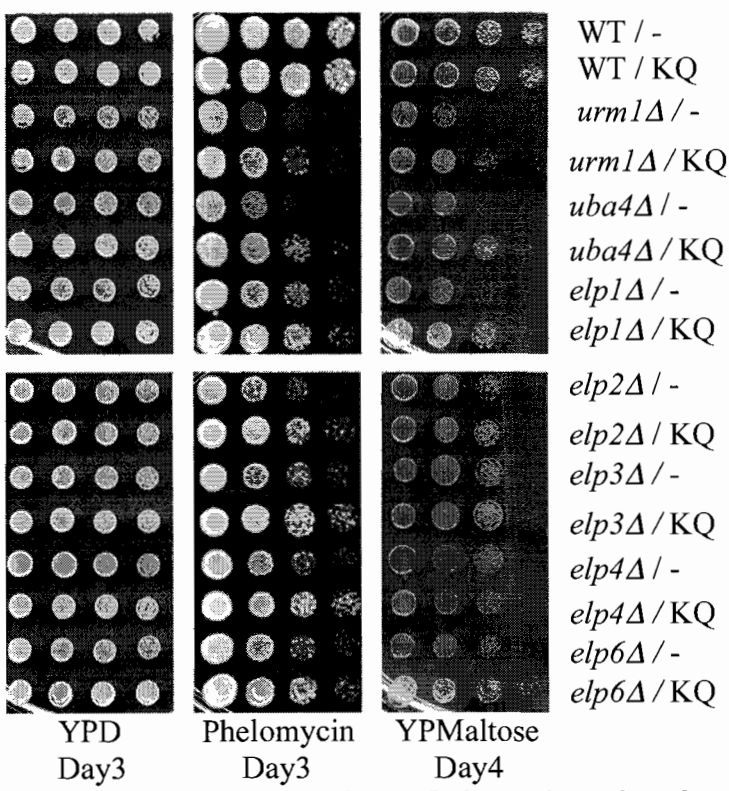

Fig. 4.11. **Urm1 and Elongator mutants growth on phelomycin and maltose media, and the over-expression of tRNAs.** BY4741 (WT) was the background strain. Strains were plated at 0.7 OD_{600} and serially diluted at 1/10 ratios. 3μg/ml Phelomycin was added to YPD plates. **A)** Sensitivity of null mutants. **B)** Strains were transformed with either the CY4035 (-) the empty plasmid or CY4034 (KQ) tRNAs.

A)

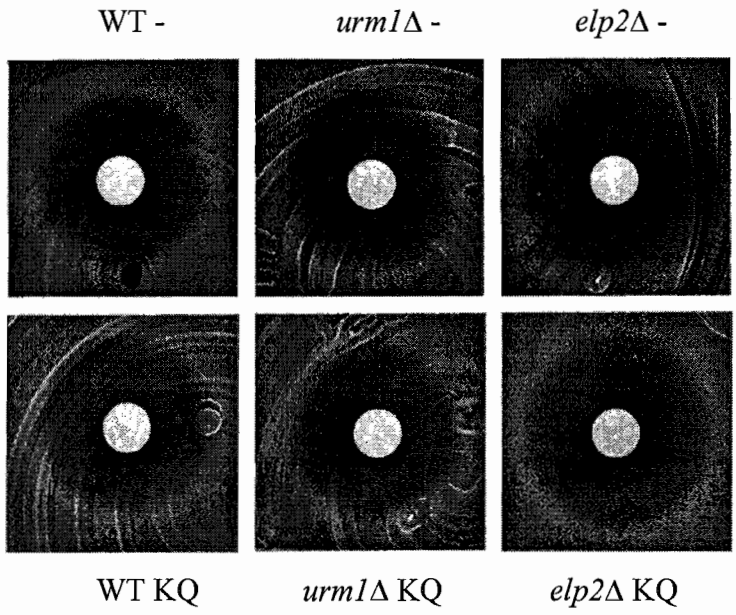

B)

	WT -	WT KQ	*urm1Δ* -	*urm1Δ* KQ	*elp2Δ* -	*elp2Δ* KQ
Diameter	19.81	20.12	21.39	19.87	22.97	21.73
Sensitivity			7%	0%	14%	7%
Suppression via tRNA		0%		7%		5%

Fig. 4.12. **Sensitivity of *urm1Δ* and *elp2Δ* mutants to LatA was suppressed by the over-expression of tRNAs.** BY4741 (WT), SY3839 (*urm1Δ*), and SY3817 (*elp2Δ*) were transformed with either the CY4035 (-) the empty plasmid or CY4034 (KQ) tRNAs then plated as described in the Materials and Methods **A)** 10μl of 1.0mM LatA was added to Whatmann discs placed on the media. Growth was measured after 5 days at 25°C. **B)** The diameter was measured in mm and represents the average of three separate experiments. Sensitivity and suppression are measured as the change in size of the halo compared to WT.

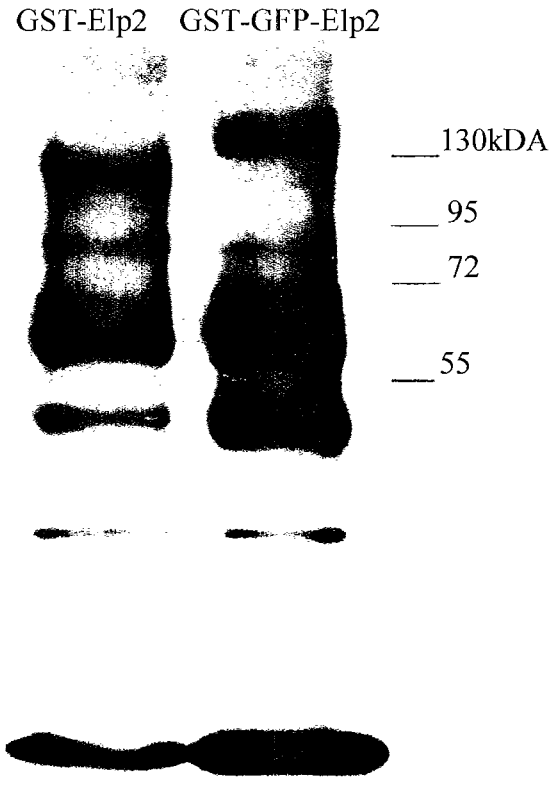

Fig. 4.13. **The Urm1 conjugation of Elp2 evidenced by western analysis.** Lysates SY4320 (WT) + CY3937 (URM1) and either CY4025 (GST-Elp2) or CY4032 (GST-GFP-Elp2) were grown in 4% selective galactose media for 6hours. Strains were then immunoprecipitated using glutathione beads, described in the Materials and Methods section. Western blots were probed with Urm1 antibodies. Urmylated GST-Elp2 125kDA, GST-GFP-Elp2 150kDA.

The urmylated form of GST-Elp2 could never be observed without over-expressing both GST-Elp2 and Urm1. Given that Urm1 acts as a sulfur carrier in tRNA modification, could the urmylation of Elp2 also be significant for modifying tRNA? Urmylation could function to mediate interactions important for the formation of the Elongator complex or could facilitate interaction of other proteins with the complex through Elp2. Both Urm1 conjugation and sulfur transfer activities require the glycine-glycine motif to operate, thereby precluding sulfur transfer if Urm1 was conjugated to a protein. On the other hand detection of the urmylated Elp2 species could be an artifact of the over-expression of both components leading to an aberrant conjugation of Urm1 to Elp2. At present, I cannot distinguish these possibilities.

Conclusion

The finding that Urm1 has a role as a sulfur carrier has called into question the functional relevance of the conjugation of proteins by Urm1. All documented phenotypes associated with an *urm1Δ* strain – temperature sensitivity, diamide and rapamcyin sensitivity, and loss of filamentous growth – be at least partially suppressed by the over-expression of tRNAs. New phenotypes of the *urm1Δ* mutant that I have identified – sensitivity to phelomycin, tergitol and LatA, and a fitness defect to poor carbon sources – can also be suppressed by tRNA over-expression. Reinforcing the connection between tRNA and the *urm1Δ* mutant phenotypes, Elongator null mutants share the phenotypes discussed above, with the exception of a fitness defect to tergitol. The sensitivity of the *elpΔ* mutants compared to that of *urm1Δ* mutants was not always uniform. The loss of Urm1 had a greater impact on sensitivity to phelomycin, and the fitness defect when grown on maltose

It is not surprising that disrupting tRNA modification can have a wide range of affects on cellular processes as the efficiently of translation may be impaired. Each of *urm1Δ* mutant phenotypes may reflect an altered translation of proteins critical for the particular cellular process. Loss of the Elongator complex will abolish three modifications of tRNA: mcm^5U_{34}, ncm^5U_{34} and $mcm^5S^2U_{34}$, but an *urm1Δ* mutant only

affects the levels of $mcm^5S^2U_{34}$ (Huang *et al.*, 2008). The *urm1Δ* mutant phenotype is equal to or more severe than *elpΔ* mutants, with the exception of temperature sensitivity, suggesting that mcm^5U_{34}, ncm^5U_{34} modifications (Figure 4.1) are not responsible for the phenotypes discussed in this chapter.

The role of Urm1 in the $mcm^5S^2U_{34}$ tRNA modification does not completely explain all the phenotypes associated with *urm1Δ* mutants. Loss of Elongator function eliminates the $mcm^5S^2U_{34}$ modification, so *elpΔ* mutants should be as sensitive to varying treatments as the *urm1Δ* mutants are. Contrary to this expectation, *urm1Δ* mutants have a greater growth defect when grown in phelomycin, tergitol and maltose conditions than do *elpΔ* mutants. The differential sensitivity to phelomycin and maltose conditions suggests that $mcm^5S^2U_{34}$ modification is involved but that the absence of Urm1 likely disrupts other cellular pathways important under these growth conditions. Sensitivity to tergitol is unique to *urm1Δ* strains, but even this phenotype is suppressed by over-expression of tRNAs, raising the possibility that unidentified tRNA modifications or other facets of tRNA physiology may depend on Urm1 but not the Elongator complex. Congruent with this observation, loss of Urm1 is synthetic lethal with the Elongator complex. This suggests that Urm1 and the Elongator complex have distinct (but related) roles as well as their shared role, tRNA modification at the U_{34} residue.

The discovery that Urm1 conjugates to Elp2 could also explain the importance of Urm1 in the modification of tRNAs. No paper to date has conclusively shown that Urm1 donates the sulfur required for the thiolation of mcm^5U_{34}. Rather, it has only been shown that loss of Urm1 prevents the formation of $mcm^5S^2U_{34}$ modifications. Nonetheless, given that Urm1 shows more similarity to *E. coli* transfer protein MoeD and given that the only know tRNA modification affected is thiolation at U_{34} it is highly likely one of Urm1's roles is to donate sulfur. However, Urm1's function as a sulfur donor does not preclude it from also functioning to conjugate proteins. Elp2 is one such potential conjugation target. The fact that the urmylated Elp2 species cannot be detected without over-expressing both components calls the significance of this observed conjugation into question. However, as presented in Chapter II, very little Ahp1 protein is urmylated at

any one time, so urmylation of Elp2 may be impossible to detect without over-expression. The exact role and function of the urmylation of Elp2 will be difficult to tease apart from Urm1's role as a sulfur donor as many of the same components are required in both processes.

APPENDIX

MATERIALS AND METHODS

Strains and Growth Conditions-The yeast strains used in this study are listed in Table A.1. Haploid *MAT***a** nonessential yeast deletion strains were purchased from Open Biosystems. The Ahp1-GFP strain was purchased from Invitrogen. Other gene deletions and the N-terminal GST tagging of Ahp1 were created by PCR (Baudin *et al.*, 1993) by using pFA6a (Longtine *et al.*, 1998; Goldstein *et al.*, 1999) plasmid series of templates. Transformation of yeast was preformed as described previously (Burke *et al.*, 2000). Knockout mutants were created by replacing the entire coding region with the indicated marker. Deletion mutants and the Ahp1-GST construct was confirmed by PCR and sequencing.

Creation of the *ptc1Δurm1Δhog1Δ* strain began with the knockout of *HOG1* via PCR (Baudin *et al.*, 1993) with the pFA6 *hphMX4* cassette (Goldstein *et al.*, 1999) in the SY4342 *ptc1Δ* strain, creating SY4453 *ptc1Δhog1Δ*. SY4453 was then mated to SY4321 *urm1Δ* and subjected to diploid selection to isolate SY4449. Tetrad dissection was preformed on SY449, as described (Buke *et al.*, 2000). SY4450 *ptc1Δurm1Δ*, SY4348 *hog1Δ urm1Δ* and SY4451 *ptc1Δhog1Δurm1Δ* were obtained from tetrads that exhibited growth on the appropriate selective media for each knockout. The relevant genotype for each strain was confirmed by PCR.

Yeast strains were propagated using standard methods (Burke *et al.*, 2000). (YP) was prepared with 1% Yeast extract (BD Diagnostic Systems), 2% Peptone (BD Diagnostic Systems). YP media containing carbon used in this study: 2% glucose (YPD), 2% Lactic Acid (YPLactic), 2% Glycerol (YPGlycerol), 2% EtOH (YPEtOH), and

2% Maltose (YPMaltose). Synthetic media was prepared with 0.67% yeast nitrogen base w/o amino acids (DIFCO), amino acids dependent on selection. The carbon added to synthetic media was then either 2% glucose (SD), 2% galactose (SGal), or 2% raffinose (SRaff). Oleate media (YPTO) was prepared by adding 1% Tergitol and 0.2% Oleate to YP media; YPT media is the same but lacking Oleate. All carbon sources are from Sigma-Aldrich. Geneticin (Research Products International Corp.), clonNAT (Werner BioAgents), Hygromycin B (A.G. Scientific, Inc.), L-Canavanine (Sigma-Aldrich), and Thialysine (Sigma-Aldrich) selection was preformed as described (Longtine *et al.*, 1998; Goldstein *et al.*, 1999; Tong *et al.*, 2006). Drugs used for the dilution series phenotypic assays: t-BOOH, diamide, rapamycin re-suspended in DMSO, and phelomycin were all from Sigma-Aldrich.

Serial dilutions were preformed by growing yeast strains over-night in appropriate liquid selective media at 30°C. The over-night cultures were then used to inoculate liquid media the following day at 0.1 OD_{600}. Strains were grown to mid-log (0.7-1.0 OD_{600}) at 30°C, washed 2X in water, and then pipetted into a 96well plate (Sarstedt) at 0.7-1.0 OD_{600} per 200µl. Each well was brought to a final volume of 200µl by the addition of water and then the cells were diluted serially. 3µl of each dilution was pipetted onto plates.

Plasmid construction- The plasmids used in this study are shown in Table A.2. Restriction enzymes used for DNA manipulations were purchased from New England Biolabs. Oligonucleotides were synthesized by Integrated DNA Technologies. Bacterial transformations and DNA preparations were preformed as previously described (Sambrook *et al.*, 1989). The template DNA for cloning genes was produced by PCR from BY4741 genomic DNA by using Vent polymerase (New England Biolabs) and the oligonucleotides listed in Table A.3. PCR product and the plasmid vector were then subjected to restriction digestion, ligated *in vitro*, and transformed into *E. coli* (Sambrook *et al.*, 1989). PVT100-U plasmid vector was used in the creation of CY3886, P_{ADH1} *AHP1*, using Ahp1-*Xba*I and Ahp1-*Bam*HI primers. PCM189 plasmid vector was used in

the creation of CY3937, P_{tetO7} *URM1*, using Urm1-*Bam*HI and Urm1-*Not*I primers. pCDBD2 plasmid vector was used in the creation of CY3925, P_{ADH1} *BD-URM1*, using Urm1-*Eco*RI and Urm1-*Cla*I primers. pGBD-C(1) plasmid vector was used in the creation of CY3950, P_{ADH1} *URM1-BD*, using Urm1-*Eco*RI and Urm1-*Cla*I primers. pGAD-C(1) plasmid vector was used in the creation of CY3952, P_{ADH1} *AD-UBA4*, using Uba4-*Eco*RI and Uba4-*Cla*I primers. Plasmids were tested by sequencing and via western analysis for expression.

Site directed mutagenesis of P_{ADH1} *AHP1* was preformed with *Pfu* Ultra polymerase (Stratagene), using primers carrying the lysine to arginine change. Template DNA was eliminated by treatment with *Dpn*I (Fisher *et al.*, 1997). Each Ahp1 mutant was confirmed by sequencing.

Sequence alignment of AHP1- Ahp1 protein sequences from *Saccharomyces cerevisiae*, *Neurospora crassa*, *Homo sapiens*, *Drosophila melanogaster*, *Arabidopsis thaliana*, *Rhodospirillum ruburm*, *Schizosaccharo pombe*, *Paracoccidioide brasiliensis*, and *Populus tremuloides* were obtained from Pubmed. Sequences were then aligned for using the ClustalW program (Thompson *et al.*, 2002).

Western blots of whole cell yeast extract - Yeast strains were grown to mid-log phase (OD_{600} ~0.7) in 10ml YPD or SD selective media at 30°C. For strains carrying $P_{GAL1/10}$*GST-6xHIS3* vectors, these cultures were then washed 2X in water and then induced in liquid SGal media for 4 hours at 30°C. Cultures were collected by centrifugation, washed once in water, and the pellet was frozen over-night. The pellet was then re-suspended in 100µl buffer A [50 mM Tris pH 8.0, 1% NP-40, 50 mM NaCl, 1 mM EDTA (all from Sigma-Aldrich)] containing a mixture of protease inhibitors [1 mM phenylmethylsulfonyl fluoride, 1 µg/ml leupeptin, 1 µg/ml pepstatin A, 1 µg/ml aprotinin, 20nM N-ethylmaleimide (all from Sigma-Aldrich)], and 1X Complete protease inhibitor mixture (Roche Diagnostics). The cells were lysed by vortexing with glass beads, and the resulting extracts were centrifuged at 12,000 x g. Protein concentration of each lysate was determined by the Bio-Rad Bradford protein assay (Bio-Rad). An equal

volume of 2X Thorner buffer [8 M urea, 5% sodium dodecyl sulfate, 40 mM Tris pH 6.8, 0.1 mM EDTA, 0.4mg/ml bromophenol blue l, β-mercaptoethanol added fresh to 1% (All from Sigma-Aldrich)] was added to the lysates and heated at 95°C for 5 minutes. Equal levels of protein sample (determined by Bradford assay) was loaded onto Bio-Rad Tris-HCl 4-15% gradient SDS-PAGE Ready Gels (Bio-Rad), subjected to electrophoresis, and electroblotted to nitrocellulose. The nitrocellulose blots were blocked for 20 minutes in 5% nonfat dried milk + TBST [10 mM Tris pH 8.0, 150 mM NaCl, 0.05% Tween 20 (all from Sigma-Aldrich)] and then incubated with appropriate antibodies in blocking buffer. For use of the Urm1 antibody, blots were exposed to 1:500 dilution of Urm1 rabbit antibody (Goerhing *et al.*, 2003) overnight at 4°C. The blots were then washed 4X in TBST and incubated in secondary anti-rabbit horse-radish peroxidase-conjugated antibody (Bio-Rad) for 1 hour at room temperature and washed 4X in TBST. Signal was then detected by Supersignal chemiluminescence (Pierce Chemical).

Glutathione S-transferase (GST) pull-down assays- Yeast strains were grown at 30°C in 100ml YPD to mid-log phase (OD_{600} ~0.7). Cultures were collected by centrifugation, washed once in water, and the yeast pellet was frozen over-night. Cell pellets were washed once in a sorbitol wash [0.3M sorbitol, 0.3M NaCl, 5mM $MgCl_2$, 10mM Tris pH 7.4 (All from Sigma-Aldrich)] then re-suspended in 400µl of lysis buffer (sorbitol wash + protease inhibiters as described above). The lysates were clarified by centrifugation at 12,000 x g, 40µl of pre-bound lysate withdrawn, and the remaining lysate was bound for to 400µl of glutathione-Sepharose 4B beads (Molecular Probes) (beads were prewashed with lysis buffer) for 1 hour rotating at 4°C .The beads were then collected by centrifugation at 500 x g, 40µl set aside for post-bound lysates, and washed 3X in lysis buffer. Protein Sample was eluated in 400µl Thorner buffer. Eluates were concentrated to 100µl by centrifugation in Ultracel YM-30 size exclusion centrifugation columns (Micron). Samples were then treated as above for western blotting. A known concentration of GST-Urm1, purified from *E. coli*, was also loaded to determine the levels of Ahp1-GST loaded. Blots were probed with Urm1 or mouse GST antibody (Novagen). The GST blot incubated with 1:5000 GST antibody for 1 hour and was then

treated with secondary anti-mouse horse-radish peroxidase-conjugated antibody at 1:10000 dilution (Bio-Rad).

Microscopy- SY4291 (Ahp1-GFP) and SY4292 (Ahp1-GFP *urm1Δ*) were grown at 30°C in liquid YPD to mid-log (OD_{600} ~0.7). Cells were then immediately examined under the microscope for normal exponentially growing conditions. When exposed to either 1.0mM diamide or 1.0mM tBOOH, which was added to mid-log cultures, the samples were examined at 10, 30, 60, 120, and 180 minutes. For growth in oleate media cells were grown to mid-log in liquid YP+ 1%Tergitol+ 0.2%oleate. To determine the location of mitochondria, DAPI staining was preformed. 2.5μg/ml DAPI (Sigma-Aldrich) was added to cells and placed on ice for 10 minutes. Cells were washed once in 1X PBS, before microscopy. Images were generated using an Axioplan 2 fluorescence microscope (Carl Zeiss) fitted with an Orca 100 digital camera (Hamamatsu).

Synthetic Lethal Screen- The synthetic lethal screen was carried out as described in Tong *et al.* 2006. The screen was carried out on Plus plates (Kreo Technologies) replicated to each corresponding step in the screen using Re-Pads (Kreo Technologies) on the Singer RoToR HAD Robot (Singer Instruments). SY4311 *urm1Δ* query strain was pinned onto a YPD plate at a density of 1536 yeast colonies per plate. The query plate was mated into the synthetic lethal array (Tong *et al.*, 2006), also at a density of 1536 (four-fold redundancy for each strain) on YPD for 1 day at 30°C. To select for diploids the cells were pinned to YPD + G418/clonNat plates for 2 days at 30°C. Diploids were then pinned onto enriched sporulation media and grown for 5 days at 22°C. After sporulation, cells were pinned to haploid selection media (SD –His/Arg/Lys + canavanine/thialysine) for 2 days 30°C. This round of selection was repeated. Then cells were pinned to haploid media + MSG (mono-sodium glutamate (Sigma-Aldrich))/G418 plates for 2 days at 30°C. Finally, cells were pinned to haploid media + (MSG/G418/clonNAT) for 2 days at 30°C to select for haploid double mutants. Strains were then scored for fitness. The screen was preformed 3 independent times. To confirm the synthetic interaction, each hit was tested individually by random spore analysis (Tong

et al., 2006). A small amount of cells was taken from the sporulation plate with a toothpick and then re-suspended in 200µl water. 20µl was plated to haploid media, 40µl was plated to either haploid media + G418 or haploid media + clonNAT, and 80µl plated to haploid media + G418/clonNAT. Plates were then incubated for 2 days at 30°C.

Two-hybrid screen- Both *URM1* bait vectors CY3925 and CY3950 were tested for self activation of the reporters in the PJ69-4A strain by growth on SD –Ade and SD –His +3mM aminotriazole (AT) (Sigma-Aldrich) media. The *lacZ* reporter was tested by growing the yeast strains on selective media for 2 days at 30°C and then replicating them to Whatman paper. The Whatman paper was exposed to -80°C for 10minutes to lyse the cells. The Whatman paper was then soaked in 3mL of in Z buffer [120mM NaP_i pH 7.0, 10mM KCl, 1mM $MgSO_4$, 20mM β-mercaptoethanol (all from Sigma-Aldrich)] + 1mg/ml X-GAL (Sigma-Aldrich) and incubated overnight at 30°C. Three activation domain plasmid libraries were used: Y2HL-C1, C2, C3 (James *et al.*, 1996). *E. coli* cells carrying the libraries were grown in 400 ml T-broth [(1.2% Bacto Tryptone (BD Diagnostics), 2.4% Bacto Yeast Extract (BD Diagnostics), 0.4% Glycerol (Sigma-Aldrich) + 200 µg/ml ampicillin (Sigma Aldrich)] to 1.5 OD_{600}. The plasmid libraries were then isolated using the Qiagen Plasmid Midi Kit (Qiagen). The transformation of each plasmid library into PJ690-4A was accomplished as described (Bartel *et al.*, 1997). The transformation was plated onto SD –His, Trp, Leu + 3mM AT media. Transformants were then tested for ability to grow on SD –Ade and expression of *lacZ* via the X-GAL assay. The plasmids from each transformant, that activated each reporter, was then isolated by the yeast plasmid rescue protocol (Burke *et al.*, 2000). Rescued plasmids were then re-transformed into PJ690-4A and re-tested for activation of reporters.

Over-expression Screen- The over-expression array (Sopko *et al.*, 2006) was pinned to SD –Leu, SGal –Leu and SGal –Leu + 1.5mM diamide Plus Plates using the Singer RoToR HAD Robot as described above. Plates were incubated at 30°C and examined daily for up to 6 days. The screen was preformed once and initial hits were

streak purified from the array and re-examined by dilution series on the same media to confirm diamide sensitivity.

TCA precipitation of phosphorylated Hog1- 10 OD_{600} of cells from mid-log cultures were pelleted by centrifugation and re-suspended in YPD or YPD + either 0.05M, 0.1M, 0.15M, or 0.2M NaCl. The re-suspended cultures were incubated at 30°C for 10 minutes. Cultures were then centrifuged and the pellets were placed on ice for 5 minutes. Each pellet was then re-suspended in 150ul of lysis buffer (1.83M NaOH, 7.2% β-mercaptoethanol) and placed back on ice for 10minutes. Following lysis, 150µl of 50% Trichloracetic Acid (Sigma-Aldrich) was added to each sample. After 10 minutes on ice, the samples were then spun down at 12,000 x g for 2 minutes and the supernatant was removed. The pellet was washed one time with 1ml ice cold Acetone and re-suspended in 100µl Thorner buffer +1mM NaVanadate (Sigma-Aldrich). Samples were boiled for 5minutes and 20µl of each sample was used for western analysis as described above. Primary blots were incubated with either 1:1000 pYHog1, phospho-P38 MAPK (Thr180, Tyr182) rabbit antibody (Cell Signaling Technology) or 1:1000 Dpm1 mouse antibody, a gift from Tom Stevens laboratory (University of Oregon, Eugene, OR).

β-galactosidase activity of STL1-lacZ- Strains were grown to mid-log phase (OD_{600} ~0.7) in 10ml SD selective media at 30°C. If salt induced, 1M NaCl was added to the culture and incubated for an additional hour at 30°C. Cultures were spun down and washed 2X in water. Pellets were then re-suspended in 100µl buffer A, minus NEM, and lysed with glass beads as described above. 1µl of each lysate was added to 150µl Z buffer + 4mg/ml CPRG (Roche) and pipetted into a 96 well plate. The plate was then read in a Tunable Microplate Reader (VersaMax) for 1 hour at 37°C. Using the SoftMax Pro software (Molecular Devices), set to kinetic program (OD_{575}/OD_{600}), an OD_{575} point during the exponential phase of CPRG conversion was converted to Miller units. Each experiment was preformed 3 separate times.

Plate washing invasive growth assay- Strains were grown to mid-log (0.7-1.0 OD_{600}) in YPD at 30°C were pipetted into a 96well plate (Sarstedt) at 0.7OD_{600} per

200µl. Each well was brought to a final volume of 200µl by the addition of water. 3µl of each dilution was pipetted onto plates. Plates were grown for 4 days at 30°C. To asses agar invasion the plates were washed under a stream of running water as the surface was gently rubbed with a gloved hand.

Latrunculin A growth study- Strains were grown to mid-log phase (OD_{600} ~0.7) in 10ml SD selective media at 30°C. 1ml of the cultures were spread on to a selective SD plate and allowed to dry. 7mm Whatman paper discs, created using a hole punch and sterilized via an autoclave, were placed on the plates. 10µl of 1.0mM LatA (Sigma-Aldrich), dissolved in DMSO, was pipetted onto the discs. Plates were then incubated at 25°C and analyzed after 6 days by measuring the diameter of the halo. A parallel set of plates with Whatman discs soaked in only 10µl of DMSO served as a negative control. The experiment was preformed three independent times.

Table A.1. **Yeast strain table**

Strain	Genotype	Reference
BY4741	*MAT***a** *his3Δ1 leu2Δ0 met15Δ0 ura3Δ0*	Open Biosystems
SY3839	BY4741 except *urm1Δ::kanMX4*	Open Biosystems
SY3840	BY4741 except *uba4Δ::kanMX4*	Open Biosystems
SY4119	BY4741 except *ahp1Δ::kanMX4*	Open Biosystems
SY4139	BY4741 expect *Ahp1-GST::kanMX4* (P_{tetO7} *URM1)*	This Study
SY4291	*MAT***a** *his3Δ1 leu2Δ0 met15Δ0 ura3Δ0 Ahp1-GFP*^{S65T}*::HIS3MX*	Invitrogen
SY4292	SY4291 except *urm1Δ::kanMX4*	This Study
PJ69-4A	*MAT***a**, *trp1-901 leu2-3,112 ura3-52 his3-200 gal4Δ gal80Δ GAL2-ADE2 LYS2::GAL1-HIS3 met2::GAL7-lacZ*	James *et al.*,1996
Y3084	*MATα can1Δ::MFA1pr-HIS3 mfα1Δ::MFα1pr-LEU2 lyp1Δ his3Δ1 ura3Δ0 leu2Δ0 met15Δ0*	Tong *et al.*, 2006
SY4321	Y3084 except *urm1Δ::natMX4*	This Study
SY4470	BY4741 except *rpl8bΔ::kanMX4*	Open Biosystems
SY4471	BY4741 except *mer1Δ::kanMX4*	Open Biosystems
SY4472	BY4741 except *yck3Δ::kanMX4*	Open Biosystems
SY4473	BY4741 except *frm2Δ::kanMX4*	Open Biosystems
SY4474	BY4741 except *slx8Δ::kanMX4*	Open Biosystems
SY4475	BY4741 except *atg11Δ::kanMX4*	Open Biosystems
SY4476	BY4741 except *ssb1Δ::kanMX4*	Open Biosystems
SY4342	BY4741 except *ptc1Δ::kanMX4*	Open Biosystems
BY4742	*MATα his3Δ1 leu2Δ0 met15Δ0 ura3Δ0*	Open Biosystems
SY4343	BY4742 except *urm1Δ::natMX4*	This study
SY4452	BY4741 except *hog1Δ::hphMX4*	This study
SY4453	BY4741 except *ptc1Δ::kanMX4 hog1Δ::hphMX4*	This study
SY4450	BY4741 except *ptc1Δ::kanMX4 urm1Δ::natMX4*	This study
SY4348	BY4741 except *hog1Δ::hphMX4 urm1Δ::natMX4*	This study
SY4449	SY4453/SY4343	This study

Table A.1. (continued).

Strain	Genotype	Reference
SY4451	BY4741 except *ptc1Δ::kanMX4 urm1Δ::natMX4 hog1Δ::hphMX4*	This study
SY4477	BY4741 except *elp1Δ::kanMX4*	Open Biosystems
SY4478	BY4741 except *elp2Δ::kanMX4*	Open Biosystems
SY4479	BY4741 except *elp3Δ::kanMX4*	Open Biosystems
SY4480	BY4741 except *elp4Δ::kanMX4*	Open Biosystems
SY4481	BY4741 except *elp6Δ::kanMX4*	Open Biosystems
Sigma	*MATα leu2-3,112 ura3-52 his3-200* pseudohyphal strain	Boone Lab
SY4394	Sigma except *urm1Δ::kanMX4*	Boone Lab
SY4393	Sigma except *uba4Δ::kanMX4*	Boone Lab
SY4364	Sigma except *elp2Δ::kanMX4*	Boone Lab
SY4374	Sigma except *elp3Δ::kanMX4*	Boone Lab
SY4372	Sigma except elp6*Δ::kanMX4*	Boone Lab
HYL333	*MAT**a** ura3-52 leu2-3,112* psuedohyphal strain	Fink Lab
SY4569	HYL333 except *urm1Δ::kanMX4*	This study

Table A.2. **Plasmid table.**

Plasmid	Description	Reference
PVT100-U	P_{ADH1} expression vector	Vernet *et al.*, 1987
CY3886	P_{ADH1} *AHP1*	This Study
CY3881	P_{ADH1} $AHP1^{K47R}$	This Study
CY3882	P_{ADH1} $AHP1^{K48R}$	This Study
CY3883	P_{ADH1} $AHP1^{K79R}$	This Study
CY3884	P_{ADH1} $AHP1^{K81R}$	This Study
CY3885	P_{ADH1} $AHP1^{K102R}$	This Study
CY3902	P_{ADH1} $AHP1^{K47R, K48R, K79R, K81R, K102R}$	This Study
CY3903	P_{ADH1} $AHP1^{K32R, K47R, K48R, K79R, K81R, K102R}$	This Study
CY3904	P_{ADH1} $AHP1^{K32R, K41R, K47R, K48R, K79R, K81R, K102R}$	This Study
CY3905	P_{ADH1} $AHP1^{K32R, K41R, K47R, K48R, K79R, K81R, K102R, K113R, K124R}$	This Study
CY3933	P_{ADH1} $AHP1^{K32R, K41R, K47R, K48R, K79R, K81R, K102R, K113R, K124R, K156R}$	This Study
pCM189	P_{tetO7} expression vector	Gari *et al.*, 1997
CY3937	P_{tetO7} *URM1*	This Study
pCDBD2	C-terminal *GAL4* DNA binding domain 2-hybrid vector	James *et al.*, 1996
pGBD-C(1)	N-terminal *GAL4* DNA binding domain 2-hybrid vector	James *et al.*, 1996
CY3925	P_{ADH1} *BD-URM1*	This Study
CY3950	P_{ADH1} *URM1-BD*	This Study
pGAD-C(1)	N-terminal *GAL4* activating binding domain 2-hybrid vector	James *et al.*, 1996
CY3952	P_{ADH1} *AD-UBA4*	This Study
CY3940	$P_{GAL1/10}$*GST-6xHIS3*	Sopko *et al.*, 2006
CY3942	$P_{GAL1/10}$*GST-6xHIS3-CRF1*	Sopko *et al.*, 2006
CY3943	$P_{GAL1/10}$*GST-6xHIS3-STE20*	Sopko *et al.*, 2006
CY3944	$P_{GAL1/10}$*GST-6xHIS3-PHO81*	Sopko *et al.*, 2006
CY3946	$P_{GAL1/10}$*GST-6xHIS3-SNX41*	Sopko *et al.*, 2006
CY3947	$P_{GAL1/10}$*GST-6xHIS3-UBX4*	Sopko *et al.*, 2006

Table A.2. (continued).

Plasmid	Description	Reference
CY3948	PGAL1/10GST-6xHIS3-MPM1	Sopko et al., 2006
CY3949	PGAL1/10GST-6xHIS3-RRI1	Sopko et al., 2006
CY4016	PSTL1 lacZ	Romelfanger/ Sprague Lab
CY4035	pRS425	Esberg et al., 2006
CY4034	pRS425-tK(UUU)-tQ(UUG)	Esberg et al., 2006
CY4025	PGAL1/10GST-6xHIS3-Elp2	Sopko et al., 2006
CY4032	PGAL1/10GST-GFP-Elp2	Landreth/ Sprague Lab

Table A.3. **Primers table. Bold**, restriction site. Underlined homology to yeast sequence. A lower case nucleic acid codes for a mutation.

Comments	Primer Sequences
Ahp1-*Xba*I	GC**TCTAGA**GCGGACGAGATGTAAGGGAAAAGC
Ahp1-*Bam*HI	CG**GGATCC**CGCTTGAAG TATACGCAGTGCC
Urm1-*Bam*HI	CG**GGATCC**CGCAATACTGATTTCTGATACTAAAACG
Urm1-*Not*I	ATAAGAAT**GCGGCCGC**TAAACTATGATTCATTCAAGCT GTACAGCAC
Urm1-*Eco*RI	G**GAATTC**CGCAATACTGATTTCTGATACTAAAACG
Urm1-*Cla*I	CC**ATCGAT**TAAACTATGATTCATTCAAGCTGTACAGCA
Uba4-*Eco*RI	G**GAATTC**AATGACTACCATCTCGAGGA
Uba4-*Cla*I	CC**ATCGAT**CTAATATTTAGGAATGGTTT
pFA6a Urm1F	TTCTGATACTAAAACGAGATAGGTTAATAGCAAAATCG GGCACATACGATTTAGGTGACAC
pFA6a Urm1R	ATATATGTAGCTGCTTCTTAAAAATTATTTGCTGCTATT TAATACGACTCACTATAGGGAG
pFA6a Hog1F	TACAACTATCGTATATAATACACATACGATTTAGGTGA CAC
pFA6a Hog1R	GGGACATTAAAAAAACACGTAATACGACTCACTATAGG GAG
47F	CAAATTAATTTCTGAAAACAgGAAGGTTATCATTACCG
47R	GTAATGATAACCTTCcTGTTTTCAGAAATTAATTTG
48F	CTGAAAACAAGAgGGTATCATTACCG
48R	GGTAATGATAACCcTCTTGTTTTCAG
79F	GGATGAATTAGTTAgGGAAAAGGAAGTTGAC
79R	CAACTTCCTTTTCCcTAACTAATTCATCC
81F	GTTAAGGAAAgGGAAGTTGACCAAGTG
81R	CTTGGTCAACTTCCcTTTCCTTAAC
102F	CAAGCGTGGGTAgGAGTTTAGGTGTTAAGG
102R	CTTAACACCTAAACTCcTAGCCCACGCTTG
32F	GAATCTTGTAgGATGCCACAAACAG
32R	CTGTTTGTGGCATCcTACAAGATTC
41F	GACTTAGTTAACAgGAAATTCCCAGC

Table A.3. (continued).

Comments	Primer Sequences
41R	GCTGGGAATTTCcTGTTAACTAAGTC
47,48F	CAAATTAATTTCTGAAAACAGGAgGGTTATCATTACCG
47,48R	CGGTAATGATAACcCTCCTGTTTTCAGAAATTAATTTG
79,81F	GGATGAATTAGTTAGGGAAAgGGAAGTTGAC
79,81R	GTCAACTTCcCTTTCCCTAACTAATTCATCC
113F	CTGTTTGTGGCATCcTACAAGATTC
113R	GGCAAACcTGATGTGTGTGGTGTCC
124F	GGCGACTACAgATTCCAATACATTGC
124R	GCAATGTATTGGAATcTGTAGTCGCC
156F	CTTACGCTGCCAgGGAAACCAACCC
156R	GGGTTGGTTTCCcTGGCAGCGTAAG

BIBLOGRAPHY

Agris, P.F. (1991). Wobble position modified nucleosides evolved to select transfer RNA codon recognition: a modified-wobble hypothesis. Biochimie. *11*, 1345-1349.

Agris, P.K. (2008). Bringing order to translation: the contributions of transfer RNA anticodon-domain modification. EMBRO Rep. *9*, 4-18.

Bach, I., and Ostendorff, H.P. (2003). Orchestrating nuclear functions: ubiquitin sets the rhythm. Trends Biochem. Sci. *4*, 189-195.

Bartel, P.L., and Fields, S. (1997). The Yeast Two-Hybrid System. Oxford, NY: Oxford University Press.

Baudin, A., Ozier-Kalogeropoulos, O., Denouel, A., Lacroute, F., and Cullin, C. (1993). A simple and efficient method for direct gene deletion in *Saccharomyces cerevisiae*. Nucleic Acids Res. *21*, 3329-3330.

Beck T., and Hall, M.N. (1999). The TOR signalling pathway controls nuclear localization of nutrient-regulated transcription factors. Nature. *402*, 689-92.

Bjork, G.R., Durand, J.M., Hagervall, T.G., Leipuviene, R., Lundgren, H.K., Nilsson, K., Chen, P., Qian, Q., and Urbonavicius, J. (1999). Transfer RNA modification: influence on translational frameshifting and metabolism. FEBS Lett. *2*, 47-51.

Bjork, G.R., Huang, B., Persson, O.P., and Bystrom, A.S. (2007). A conserved modified wobble nucleoside (mcm^5s^2U) in lysyl-tRNA is required for viability in yeast. RNA. *13*, 1245-1255.

Brewster, J.L., de Valoir, T., Dwyer, N.D., Winter, E., and Gustin, M.C. (1993). An osmosensing signal transduction pathway in yeast. Science. *259*, 1760-1763.

Burke, D., Dawson, D., and Stearns, T. (2000). Methods in Yeast Genetics, A Cold Spring Harbor Laboratory Course Manual. Cold Spring Harbor, NY: Cold Spring Harbor Laboratory Press.

Carmel-Harel, O., and Storz, G. (2000). Roles of the glutathione- and thioredoxin-dependent reduction systems in the *Escherichia coli* and *Saccharomyces cerevisiae* responses to oxidative stress. Annu. Rev. Microbiol. *54*, 439-461.

Ciechanover, A., and Schwartz, A.L. (1994). The ubiquitin-mediated proteolytic pathway: mechanisms of recognition of the proteolytic substrate and involvement in the degradation of native cellular proteins. FASEB J. *2*, 182-191.

Di Fiore, P.P., Polo, S., and Hofmann, K. (2003). When ubiquitin meets ubiquitin receptors: a signaling connection. Nat. Rev. Mol. Cell. Biol. *6*, 491-497.

Esberg, A., Huang, B., Johansson, M.J., and Bystrom, A.S. (2006). Elevated levels of two tRNA species bypass the requirement for elongator complex in transcription and exocytosis. Mol. Cell. *1*, 139-148.

Farcasanu, I.C., Hirata, D., Tsuchiya, E., Mizuta, K., and Miyakawa, T. (1999). Involvement of thioredoxin peroxidase type II (Ahp1p) of *Saccharomyces cerevisiae* in Mn2+ homeostasis. Biosci. Biotechnol. Biochem. *63*, 1871-1881.

Fields, S., and Song, O. (1989). A novel genetic system to detect protein-protein interactions. Nature. *340*, 245-246.

Fisher, C.L., and Pei, G.K. (1997). Modification of a PCR-based site-directed mutagenesis method. Biotechniques. *23*, 570-574.

Frohloff, F., Jablonowski, D., Fichtner, L., and Schaffrath, R. (2003). Subunit communications crucial for the functional integrity of the yeast RNA polymerase II elongator (gamma-toxin target (TOT)) complex. J. Biol. Chem. *278*, 956-961.

Furukawa, K., Mizushima, N., Noda, T., and Ohsumi, Y. (2000). A protein conjugation system in yeast with homology to biosynthetic enzyme reaction of prokaryotes. J. Biol. Chem. *11*, 7462-7465.

Gari, E., Piedrafita, L., Aldea, M., and Herrero, E. (1997). A set of vectors with a tetracycline-regulatable promoter system for modulated gene expression in *Saccharomyces cerevisiae*. Yeast. *13*, 837-848.

Gimeno, C.J., Ljungdahl, P.O., Styles, C.A., and Fink, G.R. (1992). Unipolar cell divisions in the yeast *S. cerevisiae* lead to filamentous growth: regulation by starvation and RAS. Cell. *6*, 1077-1090.

Goehring, A.S., Rivers, D.M., and Sprague, G.F. Jr. (2003). Urmylation: a ubiquitin-like pathway that functions during invasive growth and budding in yeast. Mol. Biol. Cell. *11*, 4329-4341.

Goehring, A.S., Rivers, D.M., and Sprague, G.F. Jr. (2003). Attachment of the ubiquitin-related protein Urm1p to the antioxidant protein Ahp1p. Eukaryot. Cell. *5*, 930-936.

Goldstein, A., and McCusker, J.H. (1999). Three new dominant drug resistance cassettes for gene disruption in *Saccharomyces cerevisiae*. Yeast. *15*, 1541-1553.

Gustin, M.C., Albertyn, M., Davenport, A., and Davenport, K. (1998). MAP kinase pathways in the yeast *Saccharomyces cerevisiae*. Microbiol. Mol. Biol. Rev. *62*, 1264-1300.

Haglund, K., Di Fiore, P.P., and Dikic, I. (2003). Distinct monoubiquitin signals in receptor endocytosis. Trends Biochem. Sci. *11*, 598-603.

Hardwick, J.S., Kuruvilla, F.G., Tong, J.K., Shamji, A.F., and Schreiber, S.L. (1999). Rapamycin-modulated transcription defines the subset of nutrient-sensitive signaling pathways directly controlled by the Tor proteins. Proc. Natl. Acad. Sci. USA. *26*, 14866-14870.

Hicke, L., Schubert, H.L., and Hill, C.P. (2005). Ubiquitin-binding domains. Nat. Rev. Mol. Cell Biol. *8*, 610-621.

Hilgarth, R.S., Murphy, L.A., Skaggs, H.S., Wilkerson, D.C., Xing, H., and Sarge, K.D. (2004). Regulation and function of SUMO modification. J. Biol. Chem. *52*, 53899-53902.

Hochstrasser, M. (2000). Biochemistry. All in the ubiquitin family. Science. *5479*, 563-564.

Hopper, A.K., and Phizicky, E.M. (2003). tRNA transfers to the limelight. Genes Dev. *17*, 162-180.

Huang, B., Johansson, J.O., and Bystrom, A.S. (2005). An early step in wobble uridine tRNA modification requires the Elongator complex. RNA. *11*, 424-436.

Huang, B., Lu, J., and Bystrom, A.S. (2008). A genome-wide screen identifies genes required for formation of the wobble nucleoside 5-methoxycarbonylmethyl-2-thiouridine in *Saccharomyces cerevisiae*. RNA. *10*, 2183-2194.

Huh, W.K., Falvo, J.V., Gerke, L.C., Carroll, A.S., Howson, R.W., Weissman, J.S., and O'Shea, E.K. (2003). Global analysis of protein localization in budding yeast. Nature. *6959*, 686-691.

Jacoby, T., Flanagan, H., Faykin, A., Seto, A.G., Mattison, C., and Ota, I. (1997). Two protein-tyrosine phosphatases inactivate the osmotic stress response pathway in yeast by targeting the mitogen-activated protein kinase, Hog1. J. Biol. Chem. *28*, 17749-17755.

James, P., Halladay, J., and Craig, E. (1996). Genomic libaries and a host strain designed for highly efficient two-hybrid selection in yeast. Genetics. *144*, 1425-1436.

Jin, R., Dobry, C.J., McCown, P.J., and Kumar, A. (2008). Large-scale analysis of yeast filamentous growth by systematic gene disruption and overexpression. Mol. Biol. Cell. *1*, 284-296.

Johansson, M.J., Esberg, A., Huang, B., Bjork, G.R., and Bystrom, A.S. (2008). Eukaryotic wobble uridine modifications promote a functionally redundant decoding system. Mol. Cell Bio. *28*, 3301-3312.

Kerscher, O., Felberbaum, R., and Hochstrasser, M. (2006). Modification of proteins by ubiquitin and ubiquitin-like proteins. Annu. Rev. Cell Dev. Biol. *22*, 159-180.

Kosower, N., and Kosower, E. (1987). Formation of Disulfies and Diamide. Methods Enzymol. *143*, 264-270.

Krogan, N.J., and Greenblatt, J.F. (2001). Characterization of a six-subunit holo-elongator complex required for the regulated expression of a group of genes in *Saccharomyces cerevisiae*. Mol. Cell. Biol. *21*, 8203-8212.

Lee, J., Spector, D., Godon, C., Labarre, J., and Toledano, M.B. (1999). A new antioxidant with alkyl hydroperoxide defense properties in yeast. J. Biol. Chem. *274*, 4537-4544.

Leidel, S., Pedrioli, P.G., Bucher, T., Brost, R., Costanzo, M., Schmidt, A., Aebersold, R., Boone, C., Hofmann, K., and Peter, M. (2009). Ubiquitin-related modifier Urm1 acts as a sulphur carrier in thiolation of eukaryotic transfer RNA. Nature. *12*, 228-232.

Liakopoulos, D., Doenges, G., Matuschewski, K., and Jentsch, S. (1998). A novel protein modification pathway related to the ubiquitin system. EMBO J. *8*, 2208-2214.

Lim, V.I. (1994). Analysis of action of wobble nucleoside modifications on codon-anticodon pairing within the ribosome. J. Mol. Biol. *1*, 8-19.

Lockshon, D., Surface, L.E., Kerr, E.O., Kaeberlein, M., and Kennedy, B.K. (2007). The sensitivity of yeast mutants to oleic acid implicates the peroxisome and other processes in membrane function. Genetics. *1*, 77-91.

Longtine, M.S., McKenzie, A., Demarini, D. J., Shah, N. G., Wach, A. Brachat, A., Philippsen, P., and Pringle, J. R. (1998). Additional modules for versatile and economical PCR-based gene deletion and modification in *Saccharomyces cerevisiae*. Yeast. *14,* 953-961.

Lu, J., Huang, B., Esberg, A., Johansson, M.J., and Bystrom, A.S. (2005). *Kluyveromyces lactis* gamma-toxin, a ribonuclease that recognizes the anticodon stem loop of tRNA. Nucleic Acid Res. *36*, 1072-1080.

Maeda, T., Takekawa, M., and Saito, H. (1995). Activation of yeast PBS2 MAPKK by MAPKKKs or by binding of an SH3-containing osmosensor. Science. *269*, 554-558.

Matunis, M.J. (2002). On the road to repair: PCNA encounters SUMO and ubiquitin modifications. Mol. Cell. *3*, 441-442.

Mizushima, N., Noda, T., Yoshimori, T., Tanaka, Y., Ishii, T., George, M.D., Klionsky, D.J., Ohsumi, M., and Ohsumi, Y. (1998). A protein conjugation system essential for autophagy. Nature. *395*, 395-398.

Nakai, Y., Nakai, M., and Hayashi, H. (2008). Thio-modification of yeast cytosolic tRNA requires a ubiquitin-related system that resembles bacterial sulfur transfer systems. J. Biol. Chem. *10*, 27469-27476.

Otero, G., Fellows, J., Li, Y., deBizemont, T., Dirac, A.M., Gustafsson, C.M., Erdjurment-Bromage, H., Tempst, P., and Svejstrup, J.Q. (1999). Elongator, a multisubunit component of a novel RNA polymerase II holoenzyme for transcriptional elongation. Mol. Cell. *3*, 109-188.

Pitterle, D.M., and Rajagopalan, K.V. (1993). The biosynthesis of molybdopterin in *Escherichia coli*. Purification and characterization of the converting factor. J. Biol. Chem. *18*, 13499-13505.

Posas, F., Chambers, J.R., Heyman, J.A., Hoeffler, J.P., de Nadal, E., and Arino, J. (2000). The transcriptional response of yeast to saline stress. J. Biol. Chem. *23*, 17249-17255.

Prouzet-Mauleon, V., Monribot-Espagne, C., Boucherie, H., Lagniel, G., Lopez, S., Labarre, J., Garin, J., and Lauquin, G.J. (2001). Identification in *Saccharomyces cerevisiae* of a new stable variant of alkyl hydroperoxide reductase 1 (Ahp1) induced by oxidative stress. J. Biol. Chem. *227*, 4823-4830.

"Pubmed." 10 September 2004. <http://www.ncbi.nlm.nih.gov/sites/entrez?db =nuccore&itool=toolbar>.

Rahl, P.B., Chen, C.Z., and Collins, R.N. (2005). Elp1p, the yeast homolog of the FD disease syndrome protein, negatively regulates exocytosis independently of transcriptional elongation. Mol. Cell. *17*, 841-853.

Rubio-Texeira, M. (2007). Urmylation controls Nil1p and Gln3p-dependent expression of nitrogen-catabolite repressed genes in *Saccharomyces cerevisiae*. FEBS Lett. *3*, 541-550.

"*Saccharomyces* Genome Database." 7 April 2008. <http://www.yeastgenome.org/ >.

Sambrook, J., Fritsch, E.F., and Maniatis, T. (1998). Molecular Cloning: A Laboratory Manual. Cold Spring Harbor, NY: Cold Spring Harbor Laboratory Press.

Schmitz, J., Cowdhury, M., Hanzelmann, P., Nimtz, M., Lee, E.Y., Schindelin, H., and Leimkuhler, S. (2008). The sulfurtransferase activity of Uba4 presents a link between Ubiquitin-like protein conjugation and activation of sulfur carrier proteins. Biochemistry. *24*, 6479-6489.

Singh, S., Tonelli, M., Tyler, R.C., Bahrami, A., Lee, M.S., and Markley, J.L. (2005). Three-dimensional structure of the AAH26994.1 protein from *Mus musculus*, a putative eukaryotic Urm1. Protein Sci. *8*, 2095-2102.

Sopko, R., Huang, D., Preston, N., Chua, G., Papp, B., Kafadar, K., Snyder, M., Oliver, S.G., Cyert, M., Hughes, T.R., Boone, C., and Andrews, B. (2006). Mapping pathways and phenotypes by systematic gene overexpression. Mol. Cell. *21*, 319-330.

Stanbrough, M., Rowen, D.W., and Magasanik, B. (1995). Role of the GATA factors Gln3p and Nil1p of *Saccharomyces cerevisiae* in the expression of nitrogen-regulated genes. Proc. Natl. Acad. Sci. USA. *21,* 9450-9454.

Taylor, S.V., Kelleher, N.L., Kinsland, C., Chiu, H.J., Costello, C.A., Backstrom, A.D., McLafferty, F.W., and Begley, T.P. (1998). Thiamin biosynthesis in Escherichia coli. Identification of this thiocarboxylate as the immediate sulfur donor in the thiazole formation. J. Biol. Chem. *26*, 16555-16560.

Thompson, J.D., Gibson, T.J., and Higgins, D.G. (2002) Multiple sequence alignment using ClustalW and ClustalX. Curr. Protoc. Bioinformatics. *23*, 2947-2948.

Thorpe, G.W., Fong, C.S., Alic, N., Higgins, V.J., and Dawes, I.W. (2004). Cells have distinct mechanisms to maintain protection against different reactive oxygen species: oxidative-stress-response genes. Proc. Natl. Acad. Sci. USA. *101*, 6564-6569.

Tong, A.H., Evangelista, M., Parsons, A.B., Xu, H., Bader, G.D., Page, N., Robinson, M., Raghibizadeh, S., Hogue, C.W., Bussey, H., Andrews, B., Tyers, M., and Boone, C. (2001). Systematic genetic analysis with ordered arrays of yeast deletion mutants. Science. *294*, 2364-2368.

Tong, A.H., and Boone, C. (2006). Synthetic genetic array analysis in *Saccharomyces cerevisiae*. Methods Mol. Biol. *313*, 171-192.

Uetz, P., Giot, L., Cagney, G., Mansfield, T.A., Judson, R.S., Knight, J.R., Lockshon, D., Narayan, V., Srinivasan, M., Pochart, P., Qureshi-Emili, A., Li, Y., Godwin, B., Conover, D., Kalbfleisch, T., Vijayadamodar, G., Yang, M., Johnston, M., Fields, S., and Rothberg, J.M. (2000). A comprehensive analysis of protein-protein interactions in *Saccharomyces cerevisiae*. Nature. *1403*, 623-627.
Vernet, T., Dignard, D., and Thomas, D. (1987). A family of yeast expression vectors containing the phage f1 intergenic region. Gene. *52*, 225-233.

Wang, X., Yan, Q., and Guan, M.X. (2007). Deletion of the MTO2 gene related to tRNA modification causes a failure in mitochondrial RNA metabolism in the yeast *Saccharomyces cerevisiae*. FEBS Lett. *581*, 4228-4234.

Warmka, J., Hanneman, J., Lee, J., Amin, D., and Ota, I. (2001). Ptc1, a type 2C Ser/Thr phosphatase, inactivates the HOG pathway by dephosphorylating the mitogen-activated protein kinase Hog1. Mol.Cell. Biol. *21*, 51-60.

Winkler, G.S., Petrakis, T.G., Ethelberg, S., Tokunaga, M., Erdjument-Bromage, H., Tempst, P., and Svejstrup, J.Q. (2001). RNA Polymerase II Elongator Holoenzyme is composed of two discret subcomplexes. J. Biol. Chem. *27*, 32743-32749.

Wittschieben, B.O., Otero, G., de Bizemont, T., Fellows, J., Erdjument-Bromage, H., Ohba, R., Li, Y., Allis, C.D., Tempst, P., and Svejstrup, J.Q. (1999). A novel histone acetyltransferase is an integral subunit of elongating RNA polymerase II holoenzyme. Mol. Cell. *4*, 123-128.

Xie, M.W., Jin, F., Hwang, H., Hwang, S., Anand, V., Duncan, M.C., and Huang, J. (2005). Insights into TOR function and rapamycin response: chemical genomic profiling by using a high-density cell array method. Proc. Natl. Acad. Sci. USA. *20*, 7215-7220.

Xu, J., Zhang, J., Wang, L., Zhou, J., Huang, H., Wu, J., Zhong, Y., and Shi, Y. (2006). Solution structure of Urm1 and its implications for the origin of protein modifiers. Proc. Natl. Acad. Sci. USA. *31*, 11625-11630.